HIV-1 antisense protein of different clades induces autophagy and associates to the autophagy factor p62

Short title: Association between HIV-1 ASP and p62-driven autophagy

Zhenlong Liu[1,3], Cynthia Torresilla[2,3], Yong Xiao[2,3], Clément Caté[2,3], Karina Barbosa[2], Éric Rassart[2,3], Shan Cen[4], and Benoit Barbeau[2,3]*

[1]Department of Chemistry, [2]Department of Biological Sciences and [3]Centre de recherche BioMed, Université du Québec à Montréal, Montréal, Canada

[4]Department of Immunology, Institute of Medicinal Biotechnology, Chinese Academy of Medical Sciences, Beijing, China

*Corresponding author:

E-MAIL: barbeau.benoit@uqam.ca (BB)

Abstract

Over recent years, strong support argues for the existence of an HIV-1 protein encoded by antisense transcripts and termed Antisense Protein (ASP). Furthermore, a recent *in silico* analysis has provided evidence for its recent appearance in the genome of HIV-1. We have previously detected ASP in various mammalian cell lines by Western blot (WB), flow cytometry and confocal microscopy analyses and reported that it induced autophagy, potentially through multimer formation. The aim of the current study was to examine autophagy induction by testing ASP from different clades, and to identify the implicated autophagy factors. We firstly confirmed that NL4.3-derived ASP was interacting with itself and that multimer formation was dependent on its amino region. Removal of this region was associated with reduced level of induced autophagy, as assessed by autophagosome formation but deletion of the most amino cysteine triplet did not totally abrogate multimer and autophagosome formation. Expression vectors of ASP from different clades were next tested and led to detection of monomers and varying levels of multimers with concomitant induced autophagy, as determined by increased LC3-II and decreased p62 (SQSTM1) levels. Through confocal microscopy, ASP was noted to co-localize with p62 and LC3-II in autophagosome-like cellular structures. CRISPR-based knock-out of ATG5, ATG7 and p62 genes led to increased stability in the levels of ASP. Furthermore, co-immunoprecipitation experiments demonstrated the interaction between p62 and ASP, which was dependent on the PB1 domain of p62. Interestingly, immunoprecipitation experiments further supported that ASP is ubiquitinated and that ubiquitination was also responsible for the modulation of its stability.

We are thus suggesting that ASP induces autophagy through p62 interaction and that its abundance is controlled by autophagy- and Ubiquitin/Proteasome System (UPS)-mediated degradation in which ubiquitin is playing an important role. Understanding the mechanisms underlying the degradation of ASP is essential to better assess its function.

48 ## Author Summary

49

50 In the present study, we provide the first evidence that a new HIV-1 protein termed ASP
51 when derived from different clades act similarly in inducing autophagy, an important cellular
52 process implicated in the degradation of excess or defective material. We have gained further
53 knowledge on the mechanism mediate the activation of autophagy and have identified an
54 important interacting partner. Our studies have important ramification in the understanding of
55 viral replication and the pathogenesis associated with HIV-1 in infected individuals. Indeed,
56 autophagy is implicated in antigen presentation during immune response and could thus be
57 rendered inefficient in infected cells, such as dendritic cells. Furthermore, a possible link with
58 HIV-1-associated Neurological Disorder (HAND) might also be a possible association with
59 the capacity of ASP to induce autophagy. Our studies are thus important and demonstrate the
60 importance in conducting further studies on this protein, as it could represent a new
61 interesting target for antiretroviral therapies and vaccine design.

Introduction

The genome of HIV-1 expresses essential genes for its replication, which include gag, pol and env, common to all replication-competent retroviruses in addition to the genes encoding regulatory proteins (Tat and Rev) crucial for virus replication. Furthermore, HIV-1 is known to encode a number of accessory proteins, i.e. Vpu, Vpr, Vif, and Nef, all of which are suggested to be implicated in the inactivation of restriction factors and the modulation of immune functions (1-6). A former study had however demonstrated that HIV-1 isolates contained a conserved open reading frame (ORF) on the antisense strand of the Env gene, thereby hinting toward the existence of a tenth gene with a encoding potential for a 189 amino acid protein (7, 8). A recent study has further underscored the high degree of conservation of this ORF in most HIV-1 clades, but further argued that this gene correlated with the spread of the virus, being less present (or absent) in most SIV, HIV-1 groups N, O and P and less prevalent HIV-1 clades (9). Importantly, a number of previous and more recent studies have further confirmed that antisense transcription overlapping this ORF sequence was detected in transfected and chronically infected cells (10-19).

The existence of the presumed encoded protein termed ASP (Antisense Protein) in infected patients has been further suggested by several groups through detection of specific antibodies and CD8+ T cell-mediated immune responses (10, 20-22). However, ASP detection itself has proven to be more difficult and was first analyzed by in *vitro* translation and electron microscopy in transfected and chronically infected cells (10, 15). More recent studies have provided a better understanding of this protein in terms of its potential membrane

localization and its biased expression in monocyte-derived macrophages and dendritic cells (7, 17). In another recent report, we have been able to clearly detect the ASP protein for the first time by Western blot and various other approaches (confocal microscopy and flow cytometry) in transfected cell lines (23). Furthermore, our work further suggested that ASP was unstable, formed multimers and induced autophagy, likely through the formation of these high molecular weight complexes.

Autophagy, a major cellular degradation pathway, plays an important role in developmental processes, cellular stress responses, and immune pathways induced by pathogens. The early step of what is known as macroautophagy initiates through mTOR inhibition and ensuing formation of an active autophagy complex consisting of the phosphorylated Beclin-1 factor, normally negatively inhibited by its binding to Bcl-2 (24-27). Following this activation, a protrusion of two lipid-based structures termed the isolation membrane and the omegasome is induced intracellularly to form the initial opened structure termed the phagophore (28). The phagophore further elongates circularly and finalizes the maturation process of the autophagosome, in which are trapped cytosolic elements targeted for degradation (27). Final fusion of the autophagosome with lysosomes leads to degradation of its content and recycling of amino acids and other constituents (29, 30). Different proteins play an active role in autophagy, such as phagophore-associated Autophagy-related-genes (ATG) ATG5, ATG7, ATG10 ATG12 and ATG16 (31). One of the classical autophagy marker is LC3-II, a phosphatidylethanolamine-modified form of LC3-I form, which is embedded in the autophagosome membrane and contribute to its formation. Another implicated autophagy marker is p62/SQSTM1, a scaffold protein, which links aggregated

107 complexes to LC3 and consequently becomes itself degraded.

108 Autophagy can either be beneficial or detrimental toward viral replication; the outcome of
109 induced autophagy depends on the virus, the cell type, and the cellular environment (32). In
110 fact, for HIV-1, initial studies in CD4+ T cells had shown that the envelope gp41 subunit
111 induced autophagy-dependent apoptosis of uninfected cells (33, 34). However, a genomic
112 screen has also identified certain autophagy-related host factors, which were rather essential
113 for HIV-1 infection (35). Furthermore, in macrophages specifically, HIV-1-induced
114 autophagy greatly improved gag pr55 processing and particle production (36). Importantly,
115 Nef has been reported to block the process of autophagy at late stages (fusion with lysosomes)
116 and avoid intracellular degradation of viral particles (5, 37). More recent data has also
117 demonstrated a potential role for other HIV-1 proteins in regulating autophagy, such as Vif
118 (38, 39).

119 Although previously associated to the proteasome degradation pathway, ubiquitination,
120 the covalent conjugation of ubiquitin to proteins, has become of high relevance to autophagy
121 (40-43). The C-terminus of ubiquitin is covalently link to the target protein by specific lysine
122 residues (e.g. K48, K63), which subsequently leads to polyubiquitination. While K48- and
123 K29-linked polyubiquitination has been shown to be optimal for degradation through the
124 proteasome, other types of lysine-linked polyubiquitinations (e.g. on K63, K11, K6) and
125 monoubiquitination may regulate processes such as autophagy, translation and DNA repair
126 (43). In fact, ubiquitinated proteins can be recognized by the autophagy pathway through
127 specialized adaptor proteins, also called sequestosome-1 like receptors (including
128 p62/SQSTM1), Optineurin and NDP52, among others). The p62 protein can multimerize via

its PB1 domain (NH_2-terminal Phox and Bem1p domain) and bind LC3-II via its LC3-interacting region (LIR) and ubiquitinated proteins through the phosphorylation of its ubiquitin-associated domain (UBA) (42-44).

Based on our previous report linking ASP to autophagy, in the current study, we aimed at examining the mechanism behind ASP-induced autophagy. Our results demonstrate that multimerization of ASP and induced autophagy partly involves its amino end. We show that ASP from various HIV-1 clades all induced autophagy, as determined by LC3-II levels and p62 degradation. We further highlight that ASP co-localized and interacted with p62 through its PB1 domain and finally present data supporting that ASP is ubiquitinated, further contributing to its targeting toward degradation pathways.

Results

Analyses of ASP multimers. A limited number of studies have shown that ASP could be detected in infected and transfected cells (15, 23). Using a codon-optimized ASP expression vector, we have successfully detected the ASP protein in transfected mammalian cells by several technical approaches, and concomitantly, demonstrated that it was forming multimers and could induce the formation of autophagosomes, thereby providing an explanation for its difficult detection (23). Herein, we sought to further define the mechanism leading to autophagy induction by ASP and to extend these analyses to ASP from different HIV-1 clades.

We were first interested in confirming the self-multimerization potential of ASP using expression vectors for Myc-tagged and chimeric GFP-optimized ASP (Fig. 1). Extracts from co-transfected 293T cells were immunoprecipitated with anti-Myc antibodies and subsequently analysed in parallel with total extracts by Western blot. As depicted in Fig. 1A, a specific signal was detected corresponding to the GFP-tagged ASP in immunoprecipitated extracts, which could not be accounted by significant difference in expression of the fusion protein in the different analysed samples. Similar co-transfection experiments were conducted in COS-7 cells and again revealed that both ASP proteins were associated (Fig. 1B). As cysteine-rich region of the protein might mediate these high molecular complexes, we pretreated the extract from Myc-tagged-ASP expressing COS-7 cells with high concentrations of reducing agents, DTT and β-mercaptoethanol. Upon treatment, the high molecular signals were strongly diminished with either agent and resulted in increased intensity of the 20 and

161 200kDs signals. Very high concentration of DTT led to disappearance of the high molecular
162 weight signals (Fig. 1C)

163 In light of these results, a series of deletion mutants were next generated, in which the
164 first 15 and 30 amino acid residues from the amino or carboxyl end of Myc-tagged ASP were
165 deleted. Importantly, pMyc-optimized-ASPΔN1-15 and pMyc-optimized-ASPΔN1-30 vectors
166 permitted the expression of an ASP mutant, from which 4 and 7 conserved cysteine residues
167 were removed, respectively (Fig. 2A). Upon transfection of COS-7 cells, flow cytometry
168 analyses showed that mutants and wild-type ASP were detected at comparative levels, except
169 for mutant pMyc-optimized-ASPΔN1-30, which showed a reduced signal (Fig. 2B). The
170 multimerization potential of these mutants were next analysed by Western blot (Fig. 2C).
171 Interestingly, the loss of the first 15 residues had an important effect on the presence of high
172 multimers, and led to a modest increase in the abundance of the monomer, while no such
173 effect was observed with mutants bearing deletion at their COOH end. The ASPΔN1-30
174 mutant presented reduced signal for both monomeric and high molecular weight signals when
175 compared to wild-type-expressing cells, which was likely due to reduced overall abundance
176 of the protein. Confocal microscopy analyses were next performed in transfected cells (Fig.
177 2D). Deletion of the first 15 amino acids reduced (but not completely abolished) the presence
178 of punctuated ASP signals, previously having been identified as autophagosomes. Deletion of
179 the carboxyl end did not lead to differences in the distribution of the resulting ASP mutant
180 from the wild-type version (Fig. 2D). Another mutant in which the conserved PXXP domain
181 (position 47-53) was also tested in transfected 293T cells and revealed no clear change in
182 multimer formation or induction of autophagy (data not shown).

Since a cysteine triplet is present in the first 15 amino acid region, we specifically deleted these cysteine residues (Fig. 3A). Flow cytometry indicated that the resulting mutant was detected at levels equivalent to those of optimized-ASP WT in transfected COS-7 cells (data not shown). Expression of the optimized ASP ΔCCC mutant in COS-7 cells resulted in a typical punctuated distribution in the cytoplasm (Fig. 3C), while Western blot analyses demonstrated that multimerization capacity of ASP ΔCCC appeared less pronounced with a concomitant increase in the monomeric signal, suggesting that this cysteine triplet was contributing to ASP multimer formation but that other cysteine (and possibly non-cysteine residues) were implicated in ASP multimerization and autophagy induction (Fig. 3B). We further tested the amino deletion mutants and the cysteine deletion mutants in 293T cells and confirmed in a clearer manner that the amino end and cysteine residues were affecting ASP multimer formation and protein levels (Fig. S1).

In light of these results, we conclude that the amino terminus (and cysteines) of ASP contribute to its capacity to multimerize, and is partly implicated in its autophagy-inducing properties.

Expression and detection of ASP from various clades. In order to better assess and understand the mechanism leading to ASP-mediated autophagy in a more representative manner, we next generated expression vectors for His-tagged ASP representing different HIV-1 clades. Importantly, these ASP ORFs were directly derived from the original proviral DNA sequence and were not codon-optimized, as we had previously performed in our earlier study (23). Sequence comparison of the ASP genes tested in this study is presented in Fig. 4A

and highlights the previously observed absence of the first 25 amino acid in clade A ASP (9). This thereby allowed us to assess the multimer formation and the autophagy-inducing capacity of an ASP version naturally missing the typical amino end. Following transfection in 293T cells, we first used our monoclonal anti-ASP antibody derived against the epitope indicated in Fig. 4A to determine if ASP could be detected by Western blot. As depicted in Fig. 4B, despite variation in the amino acid sequence of the epitope in between tested ASP, we demonstrated the presence of the expected 20 kDa signal (albeit with some variation in molecular weight and intensity between clades). Clade A ASP was detected at a lower molecular weight signal in comparison to other clade ASP, except for the 92NG083 ASP. This signal was not due to preferential usage of the internal methionine residue, as demonstrated by the similar monomeric signals observed for all tested ASP upon analyses with an anti-His antibody (Fig. 4C) but could be accounted by lower amino acid number of this ASP in the variable COOH end region. In addition, high molecular weight signals including important aggregates were detected in cells transfected with the different ASP expression vectors. Interestingly, clade A showed a more abundant monomeric form when compared to the intensity of the multimers versus ASP from other clades. A similar behavior was noted for the clade A/G ASP representative (92NG083).

These results hence showed that His-tagged ASP from different clades can be detected with anti-ASP and anti-His antibodies. Furthermore, these results confirmed that multimer formation likely involved the amino end, but that, based on the variation of multimer intensities among various tested ASP (including results with the clade A/G representative), other regions of ASP are affecting the extent of multimer formation.

Induction of autophagy by ASP from different HIV-1 clades. Since the expression of all tested ASP could be detected and led to variation in the extent of multimer formation, we were next interested in determining if these different ASP proteins could indeed induce autophagy. Based on our previous results showing that levels of the lipid-modified microtubule-associated protein 1 light chain 3 (LC3-II), a well-known autophagy marker, was increased in 293T and COS-7 cells expressing ASP (23), we used this same marker to evaluate the autophagy-inducing capacity of ASP from different clade representatives. As depicted in Fig. 5A, the presence of ASP was again confirmed for all transfected ASP vectors and was detected as monomers and multimers. Importantly, ASP from the different clades all increased levels of LC3-II, albeit to different extent in transfected 293T cells. Furthermore, based on these Western blot analyses, clade A ASP 94CY032 seemed equally capable of inducing autophagy, when compared to other ASP expression vector. We then sought to validate that this increase in LC3-II levels was related to autophagy induction and not inhibition of the late step of the autophagy, both of which would lead to increase in the abundance of LC3-II levels. Hence, transfected 293T cell were treated with Bafilomycin A1, a blocking agent of lysosomal degradation. In these conditions, ASP-dependent induced levels of LC3-II should be maintained if ASP led to induced autophagy, while no such increase should be noted if ASP inhibited the last stage of autophagy. In Figure 5B, Western blot analyses revealed that LC3-II levels were indeed increased upon Bafilomycin A1 treatment, as expected but that ASP-driven induction was also evidenced. LC3-I/LC3-II ratios in ASP-expressing cells were calculated and shown to be higher than for similarity treated

cells (-/+ Bafilomycin A1) transfected with the empty vector.

Since p62 degradation can also be used as a marker of autophagy, we conducted additional Western blot analyses in 293T cells transfected with increasing quantity of the clade B Bal ASP expression vector. A dose-dependent decrease in p62 levels was confirmed upon ASP expression, further confirming induced autophagy (Fig. 5C). Expression vectors of ASP from different clades further revealed reduced levels of p62 in transfected cells when compared to empty vector-transfected cells (Fig. S2). As a further indication of autophagy being induced by these different ASP-expressing vectors, transfected COS-7 cells were analyzed by confocal microscopy using anti-Myc antibodies. Analyses revealed the characteristic presence of cytoplasmic punctuated ASP (including cells expressing clade A ASP), which is reminiscent of autophagosomes (Fig. 5D).

These results confirmed that ASP from different clades induced autophagy and that no striking differences were noted in between clades, especially with respect to clade A ASP. They further confirmed that ASP induced autophagy, and do not suggest an inhibitory action of ASP on late stage o autophagy leading to degradation of autophagosome content.

Knockout of autophagy factors increase the abundance of ASP. Using inhibitors of early and late steps of autophagy, we have previously demonstrated that the abundance of codon-optimized NL4.3 ASP increased (23). In order to further confirm the involvement of autophagy in the regulation of ASP, we first conducted targeted knock-out of the ATG5 and ATG7 genes using the CRISPR/Cas9 system by lentivirus-mediated transduction (Fig. 6). 293T cells were first stably transduced with lentivirus expressing selective sgRNA and

following puromycin selection, two clones per knock-out were subsequently transfected with the His-tagged NL4.3 ASP expressing vector. Resulting extracts were analyzed for ASP, ATG5 and ATG7 expression. Knock-out of ATG5 or ATG7 through targeting of two different regions resulted in the reduced levels of the ATG5-ATG12 complex, although more limited for clone sgATG5-1 and, of ATG7, respectively (Fig. 6A and B). Importantly, His-tagged ASP levels increased in these clones, with a more increased abundance associated with lower expression levels of the targeted gene.

The results thereby confirmed that ASP levels in transfected cells were modulated by autophagy, and that typical autophagy factors, i.e. ATG5- ATG12 and ATG7, were implicated.

ASP interacts with autophagy factor p62. Given that all tested ASP could induce autophagy, we next investigated on the possible mechanism of action. We first focused our attention on determining whether ASP could associate and co-localize with specific autophagy factors by confocal microscopy in different cell lines (Fig. 7). As we have previously reported (23), we first confirmed that expression of NL4.3 ASP in 293T cells showed association to LC3 upon co-immunoprecipitation with anti-ASP followed by Western blot analyses (Fig. 7A). In addition, ASP was confirmed to partially co-localize with LC3-II in both COS-7 and HeLa cells (Fig. 7B and data not shown). We next performed confocal microscopy experiment to identify potential co-localization with the important autophagy protein p62. Our results revealed that a clear co-localization between ASP and p62/SQSTM1 was observed in both HeLa and 293T cells (Fig. 7C).

Since ASP forms multimers and that p62 is an important cargo transporter of multimerized proteins toward the autophagy pathway, we next tested whether ASP and p62/SQSTM1 could indeed associate. 293T cells were transfected with expression vectors of His-tagged ASP of different clades and resulting extracts were used for co-immunoprecipitation with an anti-His antibody (Fig. 7D). Upon Western blot analyses, p62 indeed could co-immunoprecipitate with ASP in transfected 293T cells. To confirm these data, immunoprecipitation was performed in similarly transfected 293T cells with anti-p62 antibodies and analyzed with anti-His antibodies (Fig. 7E). These analyses confirmed the association between ASP and p62. The specificity of this interaction was further demonstrated in transfected 293T cells by the lack of interaction of ASP with the other autophagy factors, ATG5 and ATG7 implicated in the ASP-induced autophagy cascade (Fig. S3). The impact of this association between ASP and p62 was further tested through knockout of the p62 gene in 293T cells. Although two different targeted region were tested, only one strategy (sgp62-1) provided sufficient reduction in p62 abundance. Knockout cells were thus transfected with an ASP expression vector and analyzed by Western blot. These analyses indicated that reduction in p62 levels led to a marked increase in ASP abundance (Fig. 7F).

These data thus indicated that p62 co-localized and associated to the different ASP clade representatives, and that this association might consequently lead to induction of autophagy.

Interaction domain of p62 and ASP ubiquitination. We next sought to identify the domain of p62, which was responsible for its association with ASP. These domains have been previously shown to interaction with ubiquitinated protein, LC3 and p62 itself, and termed

315 UBA, LIR and PB1, respectively (Fig. 8A). Various p62 mutants deleted for these various
316 domains and fused to the GST protein were thus co-transfected with Myc-tagged NL4.3 or
317 94CY032 (clade A) ASP expression vector in 293T cells and resulting extracts were co-
318 immunoprecipitated with anti-GST antibodies (Fig. 8B). Upon Western blot analysis of
319 immunoprecipitated extracts, interaction of ASP (monomeric and multimeric) was shown to
320 be importantly reduced in cells expressing the PB1 domain-deleted p62 mutant (Fig. 8B).
321 Expression of other mutants (deleted for LIR or UBA regions) led to retention of ASP in
322 extracts co-immunoprecipitated with anti-GST antibodies, thereby suggesting that these other
323 domains were not crucial for the association between ASP and p62. Similar results were
324 observed in immunoprecipitation experiments following co-transfection of the various p62
325 mutants and a His-tagged NL4.3 ASP expression vector in 293T cells upon Western blot
326 analyses (Fig. S4).

327 Since p62/SQSTM1 has been often implicated in ubiquitination-dependent autophagy, it
328 was surprising that the association between ASP and p62 did not involve the ubiquitinating
329 interacting domain UBA. We were thus interested in determining if ASP was nonetheless
330 ubiquitinated. Immunoprecipitation experiments were thus conducted in 293T cells co-
331 transfected with two different His-tagged ASP expression vectors (from proviral DNA clade
332 B NL4.3 and clade A 94CY032) and pRK5-HA-Ubiquitin-KOR (expressing an HA-tagged
333 ubiquitin protein limiting targeted proteins to monoubiquitination). Upon transfection of 293T
334 cells and immunoprecipitation with anti-His antibodies, Western blot analyses revealed that
335 ASP was indeed ubiquitinated, as revealed by the expected size of a ubiquitinated monomeric
336 ASP form in both clade A and clade B expressing cells (Fig. 8C). In addition, high molecular

337 weight multimers were detected in immunoprecipitated extracts. Interestingly, for both tested
338 ASP expression vectors, levels of the non-ubiquitinated form was also importantly increased
339 in transfected cells expressing ubiquitin KOR, likely suggesting that these might represent
340 non-ubiquitinated ASP protein composing ASP multimers targeted for ubiquitin-dependent
341 degradation. In fact, high molecular signals were also importantly more abundant in KOR
342 expressing cells. Further experiments using HA-tagged ubiquitin expression vectors
343 selectively producing K48 (UPS-prone) or K63 (autophagy-prone) polyuquitination revealed
344 that ASP was targeted by both of these modifications (data not shown).

345 Together, these data demonstrated that, despite the implication of the homodimerization
346 domain of p62 in its association with ASP, ASP is ubiquitinated, which impacts its abundance
347 in its monomeric and multimeric forms.
348

Discussion

Antisense transcription in HIV -1 has been described and characterized in a number of studies (18). However, the encoded ASP protein remains a limited focus of investigation. We have formerly detected ASP in different cell types by various technical approaches and further demonstrated that this viral protein led to the induction of autophagy (7, 17, 23). In the current study, we demonstrate that ASP-associated autophagy is induced in all tested clade-derived ORF and is associated to p62 via its oligomerization domain. Furthermore, ASP was shown to be ubiquitinated, which impacted on its sensitivity toward degradation.

Based on our earlier studies linking ASP-induced autophagy to its multimerization capacity, we pursued our analysis of the ASP multimers and confirmed that ASP is indeed part of multimers by showing the interaction between two differently tagged ASP. As cysteine residues can mediate multimerization, denaturing agents were tested and indeed reduced the formation of the aggregates. Furthermore, removal of the cysteine-rich amino region of ASP led to similar lower abundance of detected high molecular signals with an increase in the monomeric version, especially noted in COS-7 cells. Interestingly, as expected, the amino-truncated version was also less prone to autophagy induction. It is not clear why increase in the abundance of amino-truncated ASP mutants was not as clearly seen in 293T cells, although higher selective degradation of the codon-optimized NL4.3 ASP monomers targeted by either degradative pathways in this cell type might account for these differences. However, differences in the levels of monomeric form of ASP deleted at their amino end was further supported by the lower abundance of multimers in cells expressing clade A ASP lacking the

first 25 amino acid cysteine-rich region. These results argue that cysteine residues are implicated in the formation of these ASP multimers, which is reminiscent of other HIV-1 proteins (45, 46). Although our results argue that the cysteine triplet (position 10-12) are implicated in ASP multimer formation, we have not fully investigated on which cysteines are important but it is highly probable that various cysteine residues are involved, some of which could also lie outside of the tested regions. Furthermore, since autophagy was not completely abrogated in cells expressing amino deleted version of NL4.3 ASP, we speculate that other highly conserved regions (9) are likely to be involved in the multimerization of ASP.

In this study, a more representative assessment of the autophagy-inducing capacity was assessed through expression vectors of various ASP from various clade representatives of clinical isolates and laboratory strains. We first demonstrated for the first time that we can detect ASP from those different isolates at the expected molecular weight in transfected cells. Again, high molecular weight signals and multimers were prevalent in these analyses, albeit at different abundance, a variation potentially accountable by the absence of the cysteine-rich amino end in the case of clade A. Despite variation in multimer formation, all tested ASP induced autophagy, as determined by variation in the levels of p62 and LC3-II levels and by the presence of autophagosome-like signals by confocal microscopy. Although we have not tested all known clades (having limited out analyses to most frequent ones), our data argue for a conserved capacity of ASP from the different clade families to induce autophagy and that low abundance of multimers for certain ASP is nonetheless sufficient for this induction.

Our results thereby strongly suggest that ASP multimers in the form of potential aggregates induces autophagy and acts upon ASP abundance. This parallels similar

aggregating proteins, known to be targeted for degradation by this pathway (47, 48). We have further confirmed the implication of autophagy on the abundance of ASP by targeting known autophagy factors through CRISPR-mediated deletion. Although certain selected clones still expressed varying levels of target protein, (likely reminiscent of either more than one clone and/or single allele inactivation), resulting ASP levels (monomer and multimers) were strongly affected and their increase in abundance inversely correlated with the remaining levels of the targeted protein. We have further looked at the potential mechanisms of autophagy induction by ASP and through localisation and immunoprecipitation experiments, an association between ASP and p62 was detected, being dependent on the PB1 homodimerization domain, but not affected in a p62 mutant deleted for its ubiquitin-interacting UBA region. Interestingly, this was comparable to previous studies, in which viral proteins could interact with p62 via a ubiquitin-independent manner (49, 50). In fact, HIV-1 Tat is one of these proteins and is selectively degraded through its association to p62 via autophagy in an ubiquitin-independent manner.

These latter results are unexpected given that other experiments have revealed that ASP is ubiquitinated and that such post-translational modification contributes to ASP degradation, as demonstrated by the use of the ubiquitin mutant preventing polyubiquitination. Expression of this polyubiquitination-blocking ubiquitin protein indeed led to an important increase in abundance of the non-ubiquitinated monomeric and multimeric forms of ASP, the former likely resulting from their its in multimer complex and subsequent release upon cell extract preparation. Hence, these multimers being composed of non-ubiquitinated and ubiquitinated ASP are thus subject to degradation by autophagy through their interaction with p62.

Although it is not clear how ASP triggers autophagy, the recent publication of Lu *et al.* might shed light on the exact mechanism behind ASP-dependent induction of autophagy. The authors indeed argued that association of ubiquitinated multimeric proteins to p62 with subsequent induced autophagy is more dependent on the formation of aggregates than ubiquination itself (51). In this perspective, it is likely that the association of ASP with p62 depends on its oligomeric form and that the interaction with the ubiquitin-interacting UBA domain might not be detectable in our immunoprecipitation experiments as the association is more dependent on the multimeric form of ASP than the affinity toward ubiquitin conjugates. This is thus different from the previously suggested view that autophagy vs. UPS is mainly dependent on the type of linked ubiquitin in the polyubiquitination chain (K48 vs. K63) (52) . Our results in fact argue that both types of modification are present in monomeric and multimeric forms of ASP (data not shown).

It is well known that autophagy is primarily responsible for the degradation of most long-lived proteins in cells, but also targets aggregated proteins as well as cellular organelles and infectious organisms (53). The importance of autophagy in modulating the abundance of ASP might be crucial to maintain its abundance at low level, as this protein is likely detrimental to cell survival (if in high excess), especially given its propensity to form important multimers. In addition, the capacity of ASP to function as an inducer of autophagy also depends on other concomitantly expressed viral proteins, which have been associated to this degradation pathway (39). As previously reported, Nef can inhibit autophagy at late steps of viral replication in macrophages and could thus block ASP-induced autophagy (5, 36). Another interesting aspect of our studies relate to the essential role played by autophagy in antigen

presentation in cells, such as dendritic cells. Infected DC might thus be altered in their capacity to adequately process and present antigen, especially knowing that our previous study showed that ASP presented the highest expression in this cell type when compared to macrophages and activated CD4+ T cells (17).

Overall, our results demonstrate that the autophagy-inducing properties of ASP are observed with different clades ASP and that multimerization acts on autophagy induction. Our results further indicate that the association of p62 to ASP is likely essential for ASP and that ASP is ubiquitinated, also affecting the stability of the monomeric and multimeric forms of ASP. The body of results thereby helps to better appreciate the unstable nature of ASP in mammalian cells. The function of ASP in HIV-1 infection *in vivo* has yet to be defined but our results suggest that autophagy could link ASP to HIV-mediated pathogenesis and the chronic infection state. Future studies will be determinant in providing more information on these potential roles.

Materials and Methods

Plasmids

Expression vectors for the Myc-tagged optimized ASP and GFP-ASP optimized fusion proteins have been previously described (23). A series of deletion mutants (15 and 30 amino acids at amino or carboxyl ends) and internal deletion of cysteine triplet or PXXPXXP motif were generated by PCR from Myc-tagged optimized ASP expression vector using primers presented in Table S1. These resulted in the constructs termed pMyc-optimized-ASPΔN1-15, pMyc-optimized-ASPΔN1-30, pMyc-optimized-ASPΔC174-189, pMyc-optimized-ASPΔC159-189, pMyc-optimized-ASPΔ^{10}CCC^{12} and pMyc-optimized-ASPΔPXXP. Proviral DNA p94CY032 (clade A), NL4.3 (clade B), JR-FL (clade B), 89.6 (clade B), MJ4 (clade C), p92NG003 (clade G) and p92NG083 (clade G) were obtained through the NIH AIDS Reagent Program (Germantown MD) while proviral DNA Mal (clade D) and IndieC1 (clade C) were provided by Dr. Anne Gatignol (McGill University, Montreal, Canada). DNA fragments encoding His-tagged antisense protein (ASP) were amplified by PCR from these proviral DNA or the Bal (clade B) envelope expression vector (provided by Dr. Michel J. Tremblay, Laval University, Quebec city, Canada) using specific forward and reverse primers bearing NotI and BamHI restriction site, respectively at their 5' end. After NotI/ BamHI digestion, PCR products were inserted into the vector pTT5 (Youbio Inc. China: #VT2202,), which was similarly digested. CRISPR-Cas9 knockout plasmids (LentiCRISPRv2, Addgene: #98290 and psPAX2, AddGene: #12260) were constructed as previously described (54, 55). Pairs of oligonucleotides were designed for specificity toward targeted genes and are listed in Table

S2. Annealing of each pair further led to the generation of BsmBI restriction sites, which were used to insert the resulting dimerized oligonucleotide in the BsmBI-digested LentiCRISPRv2 vector. Plasmids pDEST-GST-P62, pDEST-GST-P62-ΔLIR, pDEST-GST-P62-ΔUBA and pDEST-GST- P62-ΔPB1 were kindly provided by Dr. Lucile Espert (Université Montpellier, Montpellier, France) and express wild-type and various deletion mutants of p62 (56). The plasmids pRK5-HA-Ubiquitin-WT (Addgene: #17608), pRK5-HA-Ubiquitin-KOR, pRK5-HA-Ubiquitin-K48 and pRK5-HA-Ubiquitin-K63 and the empty vector (Addgene #17605) were gifts from Dr. Ted Dawson (Johns Hopkins University School of Medicine, Baltimore MD) (57). The pRK5-HA-Ubiquitin WT vector expresses HA-tagged wild-type ubiquitin, while pRK5-HA-Ubiquitin-KOR expresses a ubiquitin version in which all lysines were mutated to arginine. pRK5-HA-Ubiquitin-K48 and pRK5-HA-Ubiquitin-K63 encode for ubiquitin-mutated versions in which lysine 48 and 63 respectively have been preserved, the other lysine residues having been mutated to arginine.

Cell lines and transfection

Human embryonic kidney 293T, African green monkey kidney COS-7 and human cervical HeLa cell lines were cultured in Dulbecco's modified Eagle medium (DMEM) supplemented with 10% fetal bovine serum (FBS) (Wisent Bioproducts, St-Bruno, Canada). Cell lines were obtained from the American Type Culture Collection (ATCC) (Manassas VA). All DNA plasmids were transfected using Polyethylenimine (PEI) (Polysciences, Warrington PA) at a 7:1 ratio of PEI (μg): total DNA (μg) in FBS-free DMEM: empty vectors were added to normalize DNA quantity in between transfection and for transfection control samples. After

494 an incubation of 20 min at room temperature, the PEI/DNA mixture was added to cells for 6
495 h, after which medium was removed and replaced by fresh supplemented DMEM medium. In
496 certain transfection, cells were treated with Bafilomycin A1 (100 nM) for 6 h at 24 h post-
497 transfection.
498
499 **Generation of CRISPR-Cas 9 stable cell lines**
500 Pseudotyped lentiviruses were produced by co-transfecting 293T cells with lentiCRISPRv2 or
501 lentiCRISPRv2-sgRNA (specific to ATG5, ATG7 or p62), the HIV-1 backbone-containing
502 psPAX2 and the VSV envelope encoding-pVSVg vector (Addgene: #8454) using the PEI
503 agent. At 36 h post-transfection, viral supernatants were filtered with 0.22um filters
504 (Millipore Corporation, Billerica, MA) and added to 293T and COS-7 cells. CRISPR-Cas9
505 stable knockout cell lines were selected and maintained in DMEM supplemented with 10%
506 FBS and 0.2ug/ml puromycin. Clones were generated by 10X serial dilution and single clone
507 wells were further expanded in puromycin-containing medium. Selected and amplified clones
508 were analyzed by PCR for the targeted region.
509
510 **Antibodies**
511 Anti-GST antibodies were purchased from GE Healthcare Life Science (Chicago IL). Anti-
512 Flag, anti-tubulin, anti-GAPDH, anti-LC3, anti-ATG5, anti-ATG7, anti-ATG12, anti-Beclin-1
513 and anti-p62 antibodies were purchased from Sigma-Aldrich (St-Louis MO). Antibodies
514 against Myc, His and HA tags, HRP-conjugated anti-GFP and HRP-conjugated goat anti-
515 mouse and anti-rabbit IgG antibodies were ordered from Santa Cruz Biotechnology Inc.

(Dallas TX). Mouse TrueBlot® ULTRA(Anti-Mouse Ig HRP) was purchased from Rockland Inc. (Limerick PA). Goat anti-mouse IgG coupled to Alexa Fluor 488 or to Alexa Fluor 568 were obtained from Thermo Fisher Scientific (Waltham MA). Monoclonal anti-ASP antibodies generated by Eurogentec (Liege, Belgium) were kindly provided by Dr. Jean-Michel Mesnard (Université Montpellier, Montpellier, France) and are specific to the amino acid sequence indicated in Fig. 4A.

Western blot analyses and immunoprecipitation

Cells were washed in PBS 1X and then lysed in lysis buffer (Tris 50mM pH8.0, NaCl 100mM, EDTA 1mM, 1%Triton with proteinase inhibitor (Roche, Mississauga, Canada) on ice for 15 min. In certain experiments, β-mercaptoethanol (2 %) and varying concentrations of DTT (0.1 -0.5 M) were added to the lysis buffer. The lysates were centrifuged at 2000 × *g* for 15 min at 4°C. Proteins (the supernatant) were denatured by mixing 20 µl lysates with 4X loading solution (12% sodium dodecyl sulfate (SDS) with 3 mM Tris pH 6.8 and 0.05% bromophenol blue), followed by incubation at 70°C for 10 min. For immunoprecipitation, SureBeads™ Protein G Magnetic Beads (BioRad, Hercules CA) were resuspended (20 µl per sample) and washed twice with 500 µl cold 0.1% Tween20 in PBS (PBS-T). Antibodies diluted in 500 µl PBS-T (anti-Myc (1:200), anti-p62 (1:100), anti-His (1:200), and anti-GST (1:100)) were then added to the beads for 1 hour at room temperature, and beads were next washed three times with cold PBST. Total cell extracts (lysed in 50 mM Tris–HCl pH 8, 100 mM NaCl, 1 mM EDTA and 1% Triton) were then incubated with the antibody-bead complex overnight at 4°C. After three washing with cold PBS-T, bound fractions were eluted with 20

538 µl of 2X loading buffer heated at 100°C. Samples were run on 10-12% SDS-PAGE and
539 blotted onto an Immun-Blot™ PVDF membrane (Bio-Rad Laboratories, USA) in PBS-T.
540 Membranes were blocked with 5% milk in PBS-T at room temperature for 1 h and incubated
541 with anti-ASP (1:2000), anti-GFP (1:5000), anti-Myc (1:250), anti-HA (1:10000), anti-GST
542 (1:3000) anti-His (1:5000), anti-p62 (1:2000), anti-ATG5 (1:2000), anti-ATG7 (1:2000), anti-
543 LC3 (1:500), anti-Beclin-1 (1:500), anti-GAPDH (1:1000) or anti-tubulin (1:10000),
544 antibodies at 4°C overnight. Membranes were next incubated with the appropriate HRP-
545 conjugated secondary antibodies (1 µg/ml) at room temperature for 2 h and visualized with
546 the ECL Western blotting detection kit ((Immobilon™ Western, Millipore Corporation,
547 Billerica MA). Image acquisition was performed with Fusion FX7 (Vilber Lourmat, Marne-
548 la-Vallée, France). For certain experiments, densitometric analyses were conducted on LC3-
549 related signals and a LC3-II/LC3-I ratio was calculated and normalized over cells transfected
550 with an empty vector (set at a value of 1).
551
552 **Flow cytometry**
553 Transfected COS-7 and 293T cells were washed with PBS, fixed with 4% formaldehyde for
554 10 min, and permeabilized with 0.1% Triton X-100 for 5 min at room temperature. Cells were
555 then washed three times with PBS and incubated with the anti-Myc antibody (dilution, 1:250)
556 overnight at 4°C. After three additional washes with PBS, cells were incubated with goat anti-
557 mouse IgG antibodies coupled to Alexa Fluor 488 (1/500) (Invitrogen Canada Inc) for 1 h at
558 4°C. Cells were fixed with 1% formaldehyde and incubated overnight at 4°C before analysis
559 with the FACScan device (BD Biosciences).

560

561 **Confocal microscopy**

562 COS-7 and HeLa cells were seeded in 24-well plates containing a 1.5-mm-thick coverslip for
563 12 h and then transfected, as described above. At 48 h post-transfection, cells were rinsed
564 twice with cold PBS and fixed with 4% formaldehyde/PBS for 10 min at room temperature on
565 a slow rotatory shaker. Cells were next washed with PBS/ 0.1% Triton X-100 4 times. Fixed
566 cells were incubated with a blocking solution (3% BSA, 5% milk and 50% FBS in 0.1%
567 Triton X-100, 0.05% NaN_3 PBS) overnight at 4°C, then rinsed with cold PBS three times and
568 incubated with anti-p62 (1:250), anti-ATG5 (1:250), anti-ATG7 (1:250), anti-LC3 (1:250),
569 anti-ASP (1:500), or anti-Myc (1:250) antibodies in a PBS solution containing 3% BSA, 0.1%
570 TritonX-100 and 0.05% NaN_3 at 4°C overnight. Cells were next washed with cold PBS/0.1%
571 Triton X-100 and incubated with a secondary antibody (1:500 goat anti-mouse IgG coupled to
572 Alexa Fluor 488 or goat anti-rabbit IgG coupled to Alexa Fluor 568) in the PBS solution
573 described above for 45 min. at room temperature. Cells were washed with PBS/ 0.1% Triton
574 X-100 and incubated in the immune-mount solution in the presence of 1% DAPI. All cell
575 samples were visualized with a Nikon A1 laser scanning confocal microscope (Nikon Canada,
576 Mississauga, Canada) through a 60X objective under oil immersion.
577

578 # Acknowledgments

579

580 We thank Denis Flipo for his excellent technical assistance.

581

582

583 # Reference

584

585 1. Zander K, Sherman MP, Tessmer U, Bruns K, Wray V, Prechtel AT, et al. Cyclophilin A
586 interacts with HIV-1 Vpr and is required for its functional expression. J Biol Chem.
587 2003;278(44):43202-13.

588 2. Van Damme N, Goff D, Katsura C, Jorgenson RL, Mitchell R, Johnson MC, et al. The
589 interferon-induced protein BST-2 restricts HIV-1 release and is downregulated from the cell
590 surface by the viral Vpu protein. Cell Host Microbe. 2008;3(4):245-52.

591 3. Valera MS, de Armas-Rillo L, Barroso-Gonzalez J, Ziglio S, Batisse J, Dubois N, et al.
592 The HDAC6/APOBEC3G complex regulates HIV-1 infectiveness by inducing Vif autophagic
593 degradation. Retrovirology. 2015;12:53.

594 4. Rosa A, Chande A, Ziglio S, De Sanctis V, Bertorelli R, Goh SL, et al. HIV-1 Nef
595 promotes infection by excluding SERINC5 from virion incorporation. Nature.
596 2015;526(7572):212-7.

597 5. Campbell GR, Rawat P, Bruckman RS, Spector SA. Human Immunodeficiency Virus
598 Type 1 Nef Inhibits Autophagy through Transcription Factor EB Sequestration. PLoS Pathog.
599 2015;11(6):e1005018.

600 6. Chen N, McCarthy C, Drakesmith H, Li D, Cerundolo V, McMichael AJ, et al. HIV-1
601 down-regulates the expression of CD1d via Nef. Eur J Immunol. 2006;36(2):278-86.

602 7. Clerc I, Laverdure S, Torresilla C, Landry S, Borel S, Vargas A, et al. Polarized
603 expression of the membrane ASP protein derived from HIV-1 antisense transcription in T
604 cells. Retrovirology. 2011;8:74.

605 8. Miller RH. Human immunodeficiency virus may encode a novel protein on the genomic
606 DNA plus strand. Science. 1988;239(4846):1420-2.
607 9. Cassan E, Arigon-Chifolleau AM, Mesnard JM, Gross A, Gascuel O. Concomitant
608 emergence of the antisense protein gene of HIV-1 and of the pandemic. Proc Natl Acad Sci U
609 S A. 2016;113(41):11537-42.
610 10. Vanhee-Brossollet C, Thoreau H, Serpente N, D'Auriol L, Levy JP, Vaquero C. A natural
611 antisense RNA derived from the HIV-1 env gene encodes a protein which is recognized by
612 circulating antibodies of HIV+ individuals. Virology. 1995;206(1):196-202.
613 11. Michael NL, Vahey MT, d'Arcy L, Ehrenberg PK, Mosca JD, Rappaport J, et al.
614 Negative-strand RNA transcripts are produced in human immunodeficiency virus type 1-
615 infected cells and patients by a novel promoter downregulated by Tat. Journal of virology.
616 1994;68(2):979-87.
617 12. Kobayashi-Ishihara M, Yamagishi M, Hara T, Matsuda Y, Takahashi R, Miyake A, et al.
618 HIV-1-encoded antisense RNA suppresses viral replication for a prolonged period.
619 Retrovirology. 2012;9:38.
620 13. Peeters A, Lambert PF, Deacon NJ. A fourth Sp1 site in the human immunodeficiency
621 virus type 1 long terminal repeat is essential for negative-sense transcription. Journal of
622 virology. 1996;70(10):6665-72.
623 14. Landry S, Halin M, Lefort S, Audet B, Vaquero C, Mesnard JM, et al. Detection,
624 characterization and regulation of antisense transcripts in HIV-1. Retrovirology. 2007;4:71.
625 15. Briquet S, Vaquero C. Immunolocalization studies of an antisense protein in HIV-1-
626 infected cells and viral particles. Virology. 2002;292(2):177-84.

627 16. Saayman S, Ackley A, Turner AM, Famiglietti M, Bosque A, Clemson M, et al. An HIV-
628 encoded antisense long noncoding RNA epigenetically regulates viral transcription. Mol Ther.
629 2014;22(6):1164-75.
630 17. Laverdure S, Gross A, Arpin-Andre C, Clerc I, Beaumelle B, Barbeau B, et al. HIV-1
631 antisense transcription is preferentially activated in primary monocyte-derived cells. Journal
632 of virology. 2012;86(24):13785-9.
633 18. Barbeau B, Mesnard JM. Does chronic infection in retroviruses have a sense? Trends
634 Microbiol. 2015.
635 19. Zapata JC, Campilongo F, Barclay RA, DeMarino C, Iglesias-Ussel MD, Kashanchi F, et
636 al. The Human Immunodeficiency Virus 1 ASP RNA promotes viral latency by recruiting the
637 Polycomb Repressor Complex 2 and promoting nucleosome assembly. Virology.
638 2017;506:34-44.
639 20. Anne Bet EAM, Anju Bansal, Sarah Sterrett, Antoine Gross6, Stéphanie Graff-Dubois,
640 Assia Samri, Amélie Guihot, Christine Katlama, Ioannis Theodorou, Jean-Michel Mesnard,
641 Arnaud Moris, Paul A Goepfert and Sylvain Cardinaud. The HIV-1 Antisense Protein (ASP)
642 induces CD8 T cell responses during chronic infection. Retrovirology. 2015;15(12).
643 21. Berger CT, Llano A, Carlson JM, Brumme ZL, Brockman MA, Cedeno S, et al. Immune
644 screening identifies novel T cell targets encoded by anti-sense reading frames of HIV-1.
645 Journal of virology. 2015.
646 22. Bansal A, Carlson J, Yan J, Akinsiku OT, Schaefer M, Sabbaj S, et al. CD8 T cell
647 response and evolutionary pressure to HIV-1 cryptic epitopes derived from antisense
648 transcription. J Exp Med. 2010;207(1):51-9.

649 23. Torresilla C, Larocque E, Landry S, Halin M, Coulombe Y, Masson JY, et al. Detection
650 of the HIV-1 minus-strand-encoded antisense protein and its association with autophagy.
651 Journal of virology. 2013;87(9):5089-105.
652 24. Laplante M, Sabatini DM. mTOR signaling in growth control and disease. Cell.
653 2012;149(2):274-93.
654 25. Russell RC, Tian Y, Yuan H, Park HW, Chang YY, Kim J, et al. ULK1 induces
655 autophagy by phosphorylating Beclin-1 and activating VPS34 lipid kinase. Nature cell
656 biology. 2013;15(7):741-50.
657 26. Nazarko VY, Zhong Q. ULK1 targets Beclin-1 in autophagy. Nature cell biology.
658 2013;15(7):727-8.
659 27. Wrighton KH. Autophagy: Kinase crosstalk through beclin 1. Nat Rev Mol Cell Biol.
660 2013;14(7):402-3.
661 28. Matsunaga K, Saitoh T, Tabata K, Omori H, Satoh T, Kurotori N, et al. Two Beclin 1-
662 binding proteins, Atg14L and Rubicon, reciprocally regulate autophagy at different stages.
663 Nature cell biology. 2009;11(4):385-96.
664 29. Hyttinen JM, Niittykoski M, Salminen A, Kaarniranta K. Maturation of autophagosomes
665 and endosomes: a key role for Rab7. Biochim Biophys Acta. 2013;1833(3):503-10.
666 30. Nakamura S, Yoshimori T. New insights into autophagosome-lysosome fusion. Journal
667 of cell science. 2017;130(7):1209-16.
668 31. Mizushima N, Yoshimori T, Ohsumi Y. The role of Atg proteins in autophagosome
669 formation. Annu Rev Cell Dev Biol. 2011;27:107-32.
670 32. Jackson WT. Viruses and the autophagy pathway. Virology. 2015.

671 33. Espert L, Denizot M, Grimaldi M, Robert-Hebmann V, Gay B, Varbanov M, et al.
672 Autophagy is involved in T cell death after binding of HIV-1 envelope proteins to CXCR4. J
673 Clin Invest. 2006;116(8):2161-72.
674 34. Denizot M, Varbanov M, Espert L, Robert-Hebmann V, Sagnier S, Garcia E, et al. HIV-1
675 gp41 fusogenic function triggers autophagy in uninfected cells. Autophagy. 2008;4(8):998-
676 1008.
677 35. Brass AL, Dykxhoorn DM, Benita Y, Yan N, Engelman A, Xavier RJ, et al.
678 Identification of host proteins required for HIV infection through a functional genomic
679 screen. Science. 2008;319(5865):921-6.
680 36. Kyei GB, Dinkins C, Davis AS, Roberts E, Singh SB, Dong C, et al. Autophagy pathway
681 intersects with HIV-1 biosynthesis and regulates viral yields in macrophages. J Cell Biol.
682 2009;186(2):255-68.
683 37. Shoji-Kawata S, Sumpter R, Leveno M, Campbell GR, Zou Z, Kinch L, et al.
684 Identification of a candidate therapeutic autophagy-inducing peptide. Nature.
685 2013;494(7436):201-6.
686 38. Borel S, Robert-Hebmann V, Alfaisal J, Jain A, Faure M, Espert L, et al. HIV-1 viral
687 infectivity factor interacts with microtubule-associated protein light chain 3 and inhibits
688 autophagy. AIDS. 2015;29(3):275-86.
689 39. Liu Z, Xiao Y, Torresilla C, Rassart E, Barbeau B. Implication of Different HIV-1 Genes
690 in the Modulation of Autophagy. Viruses. 2017;9(12).
691 40. Lippai M, Low P. The role of the selective adaptor p62 and ubiquitin-like proteins in
692 autophagy. Biomed Res Int. 2014;2014:832704.

693 41. Kirkin V, McEwan DG, Novak I, Dikic I. A role for ubiquitin in selective autophagy.
694 Mol Cell. 2009;34(3):259-69.
695 42. Schreiber A, Peter M. Substrate recognition in selective autophagy and the ubiquitin-
696 proteasome system. Biochim Biophys Acta. 2014;1843(1):163-81.
697 43. Miranda M, Sorkin A. Regulation of receptors and transporters by ubiquitination: new
698 insights into surprisingly similar mechanisms. Mol Interv. 2007;7(3):157-67.
699 44. Dinkins C, Pilli M, Kehrl JH. Roles of autophagy in HIV infection. Immunol Cell Biol.
700 2015;93(1):11-7.
701 45. Yuan W, Craig S, Yang X, Sodroski J. Inter-subunit disulfide bonds in soluble HIV-1
702 envelope glycoprotein trimers. Virology. 2005;332(1):369-83.
703 46. Bischerour J, Leh H, Deprez E, Brochon JC, Mouscadet JF. Disulfide-linked integrase
704 oligomers involving C280 residues are formed in vitro and in vivo but are not essential for
705 human immunodeficiency virus replication. Journal of virology. 2003;77(1):135-41.
706 47. Kragh CL, Ubhi K, Wyss-Coray T, Masliah E. Autophagy in dementias. Brain pathology.
707 2012;22(1):99-109.
708 48. Gatica D, Lahiri V, Klionsky DJ. Cargo recognition and degradation by selective
709 autophagy. Nature cell biology. 2018;20(3):233-42.
710 49. Orvedahl A, MacPherson S, Sumpter R, Jr., Talloczy Z, Zou Z, Levine B. Autophagy
711 protects against Sindbis virus infection of the central nervous system. Cell Host Microbe.
712 2010;7(2):115-27.
713 50. Sagnier S, Daussy CF, Borel S, Robert-Hebmann V, Faure M, Blanchet FP, et al.
714 Autophagy restricts HIV-1 infection by selectively degrading Tat in CD4+ T lymphocytes.

715 Journal of virology. 2015;89(1):615-25.

716 51. Lu K, den Brave F, Jentsch S. Receptor oligomerization guides pathway choice between
717 proteasomal and autophagic degradation. Nature cell biology. 2017;19(6):732-9.

718 52. Khaminets A, Behl C, Dikic I. Ubiquitin-Dependent And Independent Signals In
719 Selective Autophagy. Trends in cell biology. 2016;26(1):6-16.

720 53. Glick D, Barth S, Macleod KF. Autophagy: cellular and molecular mechanisms. J Pathol.
721 2010;221(1):3-12.

722 54. Koike-Yusa H, Li Y, Tan EP, Velasco-Herrera Mdel C, Yusa K. Genome-wide recessive
723 genetic screening in mammalian cells with a lentiviral CRISPR-guide RNA library. Nat
724 Biotechnol. 2014;32(3):267-73.

725 55. Shalem O, Sanjana NE, Hartenian E, Shi X, Scott DA, Mikkelsen TS, et al. Genome-
726 scale CRISPR-Cas9 knockout screening in human cells. Science. 2014;343(6166):84-7.

727 56. Sagnier S, Daussy CF, Borel S, Robert-Hebmann V, Faure M, Blanchet FP, et al.
728 Autophagy restricts HIV-1 infection by selectively degrading Tat in CD4+ T lymphocytes.
729 Journal of virology. 2014.

730 57. Lim KL, Chew KC, Tan JM, Wang C, Chung KK, Zhang Y, et al. Parkin mediates
731 nonclassical, proteasomal-independent ubiquitination of synphilin-1: implications for Lewy
732 body formation. J Neurosci. 2005;25(8):2002-9.

733

734

735

736

737 **Figure legends**

738

739 **Figure 1: Multimerization of ASP involves disulfide bonds. A-B**. 293T (A) and COS-7 (B)
740 cells were transfected with expression vectors for GFP-optimized-ASP, Myc-tagged-
741 optimized-ASP and/or the empty vector pcDNA3.1. At 48 h post transfection,
742 immunoprecipitation was performed using the anti-Myc antibody and Western blot analyses
743 were conducted through anti-GFP and anti-Myc antibodies. Total cellular extracts were
744 similarly analysed in parallel with an anti-GFP antibody. **C**. Extracts from COS-7 cells
745 transfected with the Myc-tagged optimized ASP expression vector (vs. pcDNA3.1) were
746 treated with of DTT and/or β-mercaptoethanol prior to Western blot analyses with anti-Myc
747 and anti-GAPDH antibodies. Both stacking and resolving gels are depicted and high
748 molecular weight (including 200 kDa multimers) vs. monomeric 20kDa ASP signals are
749 indicated.

750

751 **Figure 2: The amino end of ASP is implicated in its multimerization, A**. Schematic
752 representation of the different domains of ASP and the generated deletion mutants targeting
753 the first 15 or 30 amino acids of either the N- or C-terminal of ASP. **B-D**. COS-7 cells were
754 transfected with expression vectors for these different ASP mutants and the wild-type version
755 vs. pcDNA3.1 (empty vector) and, at 48 h post-transfection, were analysed with an anti-Myc
756 antibody by flow cytometry (**B**) and confocal microscopy (60X objective and with numerical
757 aperture of 1.4) (**C**). Cells analysed by confocal microscopy were also stained for their nuclei
758 with Hoechst. Cellular extracts from these transfected cells were also analysed by Western
759 Blot using anti-Myc and anti-GAPDH antibodies (**D**). High molecular weight (including 200

760 kDa multimers) vs. monomeric 20kDa ASP signals are indicated.

761

762 **Figure 3: Deletion of the first cysteine triplet of ASP reduces multimer formation and**
763 **autophagosome signals. A**. Schematic representation of the different domains of ASP and
764 the deletion mutant of the first cysteine triplet (^{10}CCC^{12}). **B-C**. COS-7 cells were transfected
765 with expression vectors for wild-type or cysteine triplet-deleted ASP vs. pcDNA3.1 (empty
766 vector). After 48h of transfection, using anti-Myc antibodies, cellular extracts were analysed
767 by Western Blot (**B**) and confocal microscopy (60X objective and with numerical aperture of
768 1.4) (**C**). Cells analysed by confocal microscopy were also stained for their nuclei with
769 Hoechst. High molecular weight (including 200 kDa multimers) vs. monomeric 20kDa ASP
770 signals are indicated.

771

772 **Figure 4. ASP from different clade representatives form detectable multimers. A.**
773 Sequence alignment of the predicted amino acid of ASP from different HIV-1 isolates
774 representing different clades. The peptide region used to generate anti-ASP monoclonal
775 antibodies is highlighted over the sequence from amino acid 47 to 61. **B-C.** Expression
776 vectors of His-tagged ASP from various HIV clades were transfected in 293T cells and cell
777 lysates were subsequently analyzed by Western blot for ASP (**B**: anti-ASP and **C**: anti-His).
778 Depicted on the right side of the panels are multimers and high molecular weight and
779 monomeric 20kDa ASP signals. Clade type for each tested ASP is indicated on top of each
780 lane.

781 **Figure 5. ASP from different clade representatives induce autophagy. A-B.** Expression

782 vectors of His-tagged ASP from various HIV clades and the empty vector were transfected in
783 293T cells and cell lysates were analyzed by Western blot for the detection of ASP (anti-His),
784 LC3-II levels (anti-LC3) and tubulin. Signals for LC3-I, LC3-II and ASP are indicated on the
785 left of each panel. In panel B, after transfection, cells were treated with DMSO (-) or with 100
786 nM Bafilomycin A1 (+) (Baf A1) for 6 h. LC3-II/LC3-I ratios are indicated for each lane and
787 are representative of fold value over the calculated ratio for untreated cells transfected with
788 the empty vector. **C.** Increasing quantity of clade 89.6 ASP expression vector was transfected
789 in 293T cells and cell lysates were analyzed by Western blot for ASP, p62 and tubulin. **D.**
790 COS-7 cells were transfected with expression vectors of Myc-tagged ASP from various
791 clades. After fixation, cells were labeled with anti-Myc antibodies followed by goat anti-
792 mouse IgG coupled to Alexa Fluor 488, stained with DAPI and observed by confocal
793 microscopy.
794
795 **Figure 6. Suppressed expression of ATG5 and ATG7 leads to increased ASP expression.**
796 Two different 293T cell clones knocked out for either ATG5 (sgATG5-1 and sgATG5-2) (A)
797 or ATG7 (sgATG7-1 and sgATG7-2) (B) and control stably transfected clones were
798 transfected with an His-tagged NL4.3 ASP expression vector.. Cell lysates were prepared and
799 analyzed by Western blot using anti-His, anti-ATG-5, anti-ATG7 and anti-tubulin antibodies.
800 Monomeric and multimeric signals are representing different ASP signals. The signal for
801 ATG5 is shown as the typical covalently linked ATG5-ATG12 complex.
802

Figure 7. Association between ASP and p62 with and effect of knock out p62 expression on ASP levels. **A.** 293T cells were transfected with expression vectors for optimized NL4.3 ASP or the empty vector pcDNA3.1. After 48 h post transfection, immunoprecipitation was performed using the anti-ASP antibody and Western blot analyses were conducted through anti-ASP and anti-LC3 antibodies. The Mouse TrueBlot® ULTRA (Anti-Mouse Ig HRP) (for ASP) was used as secondary antibody for Western blot analyses. **B.** Expression vectors pcDNA-opt-ASP and GFP-LC3 were transfected in COS-7 cells. After fixation and nuclei staining with DAPI, ASP was detected with anti-ASP antibodies followed by a goat anti-mouse IgG antibody coupled to Alexa Fluor 568, while LC3 detection was performed with an anti-LC3 antibody followed by a goat anti-rabbit IgG antibody coupled to Alexa Fluor 568. **C.** Expression vectors for NL4.3-ASP were transfected in COS-7 (upper panels) and HeLa (bottom panels) cells. Nuclei were stained with DAPI, and ASP was detected with anti-ASP antibodies followed by goat anti-mouse IgG antibodies coupled to Alexa Fluor 568 (COS-7) or Alexa Fluor 488 (HeLa), while p62 was detected by an anti-p62 antibodies followed by goat anti-rabbit IgG antibodies coupled to Alexa Fluor 488 (COS-7) or Alexa Fluor 568. **D-E.** Expression vectors of His-tagged ASP of various HIV clades were transfected in 293T cells and after 48 h, cellular extracts were used for immunoprecipitation with the anti-His (**D**) or anti p62 antibodies (**E**). Immunoprecipitated samples and total extracts were analyzed by Western blot using anti-p62, anti-His and anti-tubulin antibodies. **F.** 293T cell clone knocked out for p62 (sgp62) and control stably transfected clone were transfected with His-tagged NL4.3 ASP expression vector. Cell lysates were prepared and analyzed by Western blot using anti-His, anti-p62 and anti-tubulin antibodies. Monomeric and multimeric signals are

825 representing different ASP signals.

826

827 **Figure 8. The interaction of p62 with ASP requires its homodimerization domain despite**
828 **ASP ubiquitination. A.** The various domains of the p62 protein are depicted and include the
829 ubiquitination-binding domain UBA, the LC3-binding domain LIR, NLS and NES regions
830 and the homodimerization domain PB1. **B.** 293T cells were co-transfected with expression
831 vectors for GST-tagged wild-type and deletion mutants of p62 and of Myc-tagged-NL4.3
832 ASP. At 48 h post transfection, immunoprecipitation was performed using the anti-GST
833 antibody and Western blot analyses of immunoprecipitated samples along with total extracts
834 were conducted through anti-GST, anti-Myc and anti-tubulin antibodies. **C.** 293T cells were
835 co-transfected with expression vectors for His-tagged NL4.3 or 94CY032 ASP and for the
836 HA-tagged Ubiquitin-KOR mutant (restricted to monoubiquitination). At 48 h post
837 transfection, immunoprecipitation was performed with anti-His antibodies and Western blot
838 analyses of immunoprecipitated samples along with total extracts were conducted through
839 anti-His, anti-HA and anti-tubulin antibodies. Arrows on the right side of the right panels
840 indicated the position and expected MW (25-30 kDa) of the ubiquitinated ASP from the
841 different tested proviral DNA.

842

843

844

845

Table S1. Primers used for generation of ASP deletion mutants. Primers are presented as forward and reverse pairs suitable for the generation of the deletion mutants by inverse PCR, as described in Material and Methods.

Table S2: Primers for generation of expression vectors for CRISPR-mediated knockout of ATG5, ATG7, ATG12 and p62 genes. Complementary oligonucleotides are depicted for each targeted gene and were inserted tin the lentiviral vector, as indicated in Material and Methods.

Figure S1. Amino deletion and removal of a cysteine triplet in the amino end of ASP increase abundance of its monomeric form. COS-7 cells were transfected with expression vectors for ASP mutants (see Fig. 2A and 3A) or the wild-type version vs. pcDNA3.1 (mock). At 48 h post-transfection, cellular extracts were analysed by Western Blot using anti-ASP and anti-tubulin antibodies.

Figure S2. Expression of ASP from different clades leads to reduced levels of p62. . Expression vectors for His-tagged ASP from NL4.3, 94CY032, IndieC1 and Mal proviral DNA (vs. empty vector) were transfected in 293T cells and cell lysates were analyzed by Western blot for ASP (anti-His), p62 and tubulin. Clades of origin of the different tested ASP representative are indicated above each lane.

867 **Figure S3. Absence of association between ASP and the ATG5-ATG12 complex or**
868 **ATG7.** The expression vector for His-tagged NL4.3 ASP (vs. empty vector) was transfected
869 in 293T cells and at 48 h post-transfection, cellular extracts were used for
870 immunoprecipitation with anti-His antibodies Immunoprecipitated samples and total extracts
871 were analyzed by Western blot using, anti-His, anti-ATG5, anti-ATG7 and anti-tubulin
872 antibodies.

873

874 **Figure S4. Interaction of p62 with ASP requires its homodimerization domain.** 293T
875 cells were co-transfected with expression vectors for GST-tagged wild-type and deletion
876 mutants of p62 and for His-tagged-NL4.3 ASP. At 48 h post transfection,
877 immunoprecipitation was performed using the anti-GST antibody and Western blot analyses
878 of immunoprecipitated samples along with total extracts were conducted through anti-GST,
879 anti-His and anti-tubulin antibodies.

880

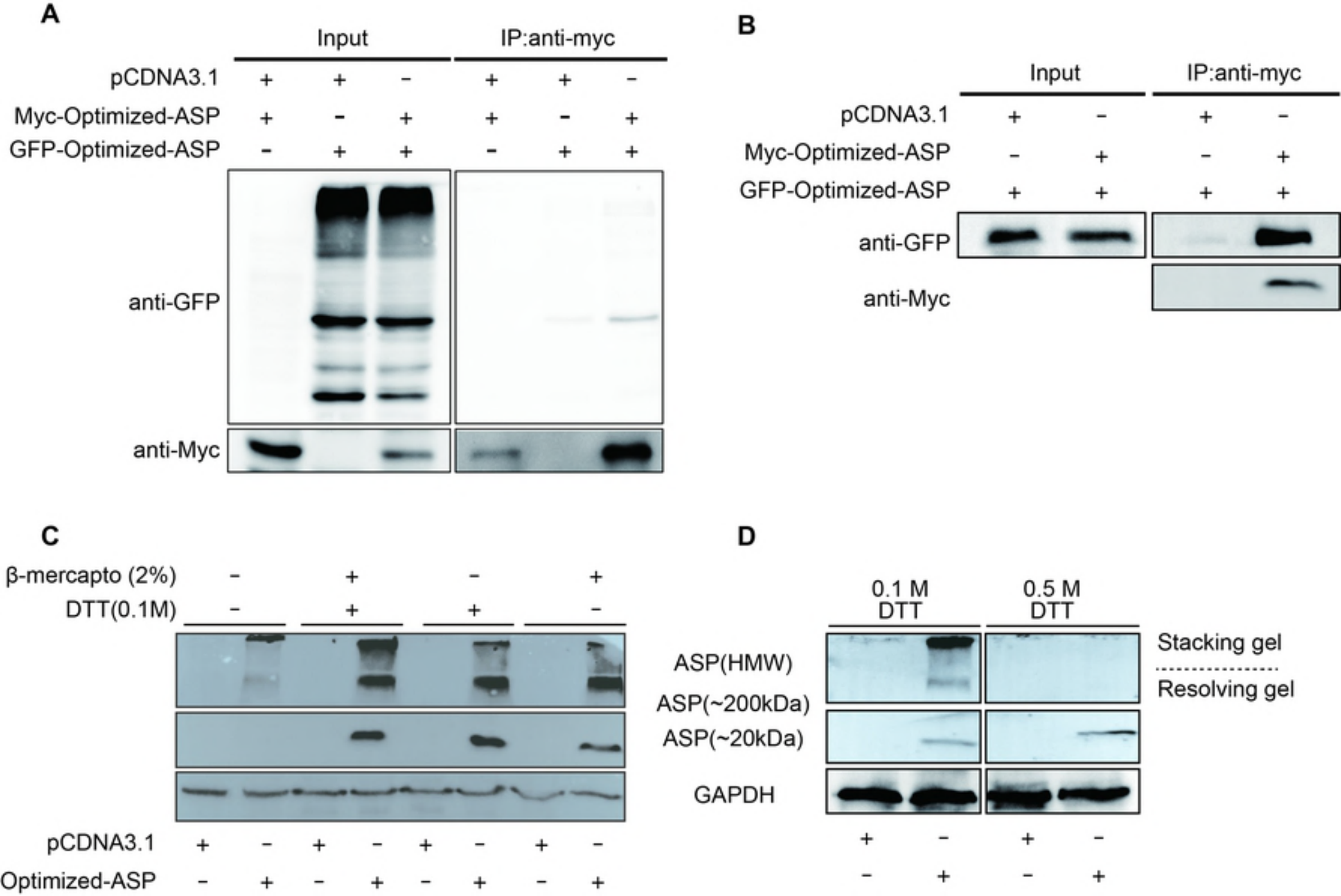
A
Input
IP:anti-myc
pCDNA3.1
Myc-Optimized-ASP
GFP-Optimized-ASP
anti-GFP
anti-Myc
B
Input
IP:anti-myc
pCDNA3.1
Myc-Optimized-ASP
GFP-Optimized-ASP
anti-GFP
anti-Myc
C
β-mercapto (2%)
DTT(0.1M)
pCDNA3.1
Optimized-ASP
D
0.1 M DTT
0.5 M DTT
ASP(HMW)
ASP(~200kDa)
ASP(~20kDa)
GAPDH
Stacking gel
Resolving gel

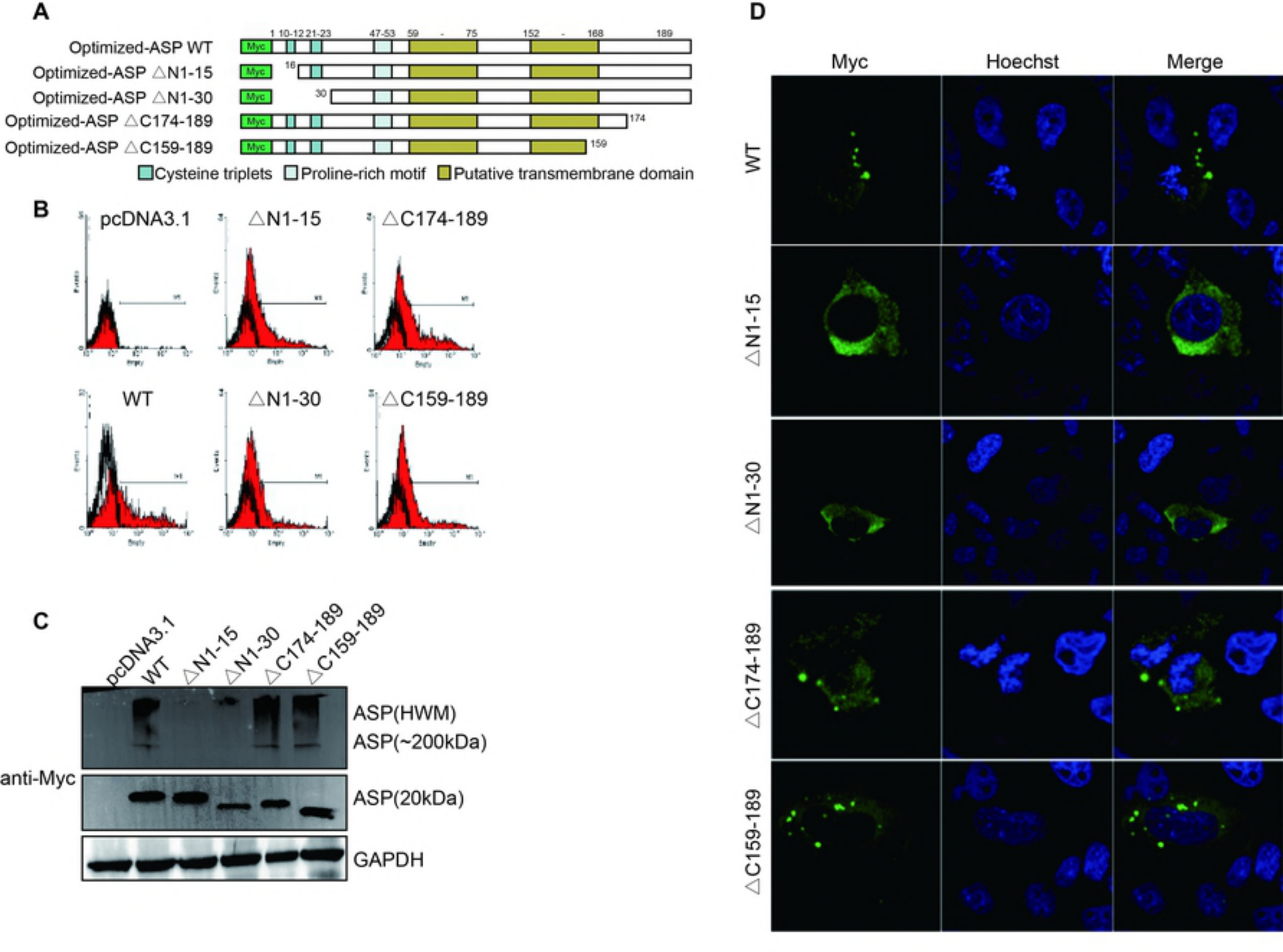
A
1 10-12 21-23 47-53 59 - 75 152 - 168 189
Optimized-ASP WT
Optimized-ASP △N1-15
Optimized-ASP △N1-30
Optimized-ASP △C174-189
Optimized-ASP △C159-189
Myc
16
30
174
159
Cysteine triplets
Proline-rich motif
Putative transmembrane domain
B
pcDNA3.1
△N1-15
△C174-189
WT
△N1-30
△C159-189
C
pcDNA3.1
WT
△N1-15
△N1-30
△C174-189
△C159-189
anti-Myc
ASP(HWM)
ASP(~200kDa)
ASP(20kDa)
GAPDH
D
Myc
Hoechst
Merge
WT
△N1-15
△N1-30
△C174-189
△C159-189

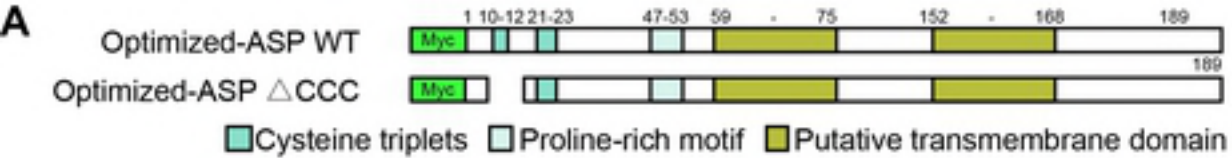
A
Optimized-ASP WT
Optimized-ASP △CCC
Myc
1 10-12 21-23 47-53 59 75 152 168 189
189
Cysteine triplets
Proline-rich motif
Putative transmembrane domain

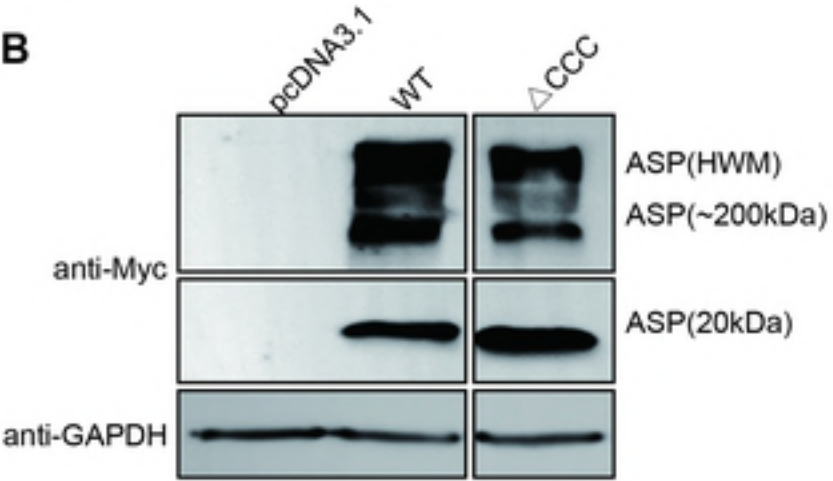
B
pcDNA3.1
WT
△CCC
ASP(HWM)
ASP(~200kDa)
ASP(20kDa)
anti-Myc
anti-GAPDH

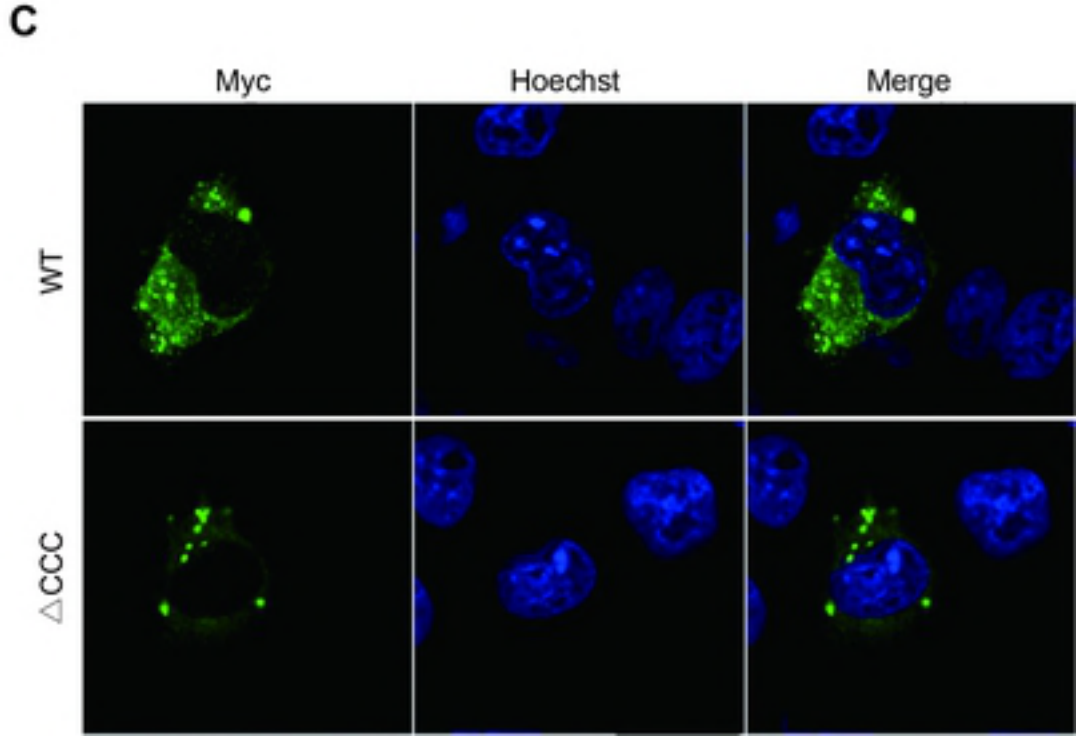
C
Myc
Hoechst
Merge
WT
△CCC

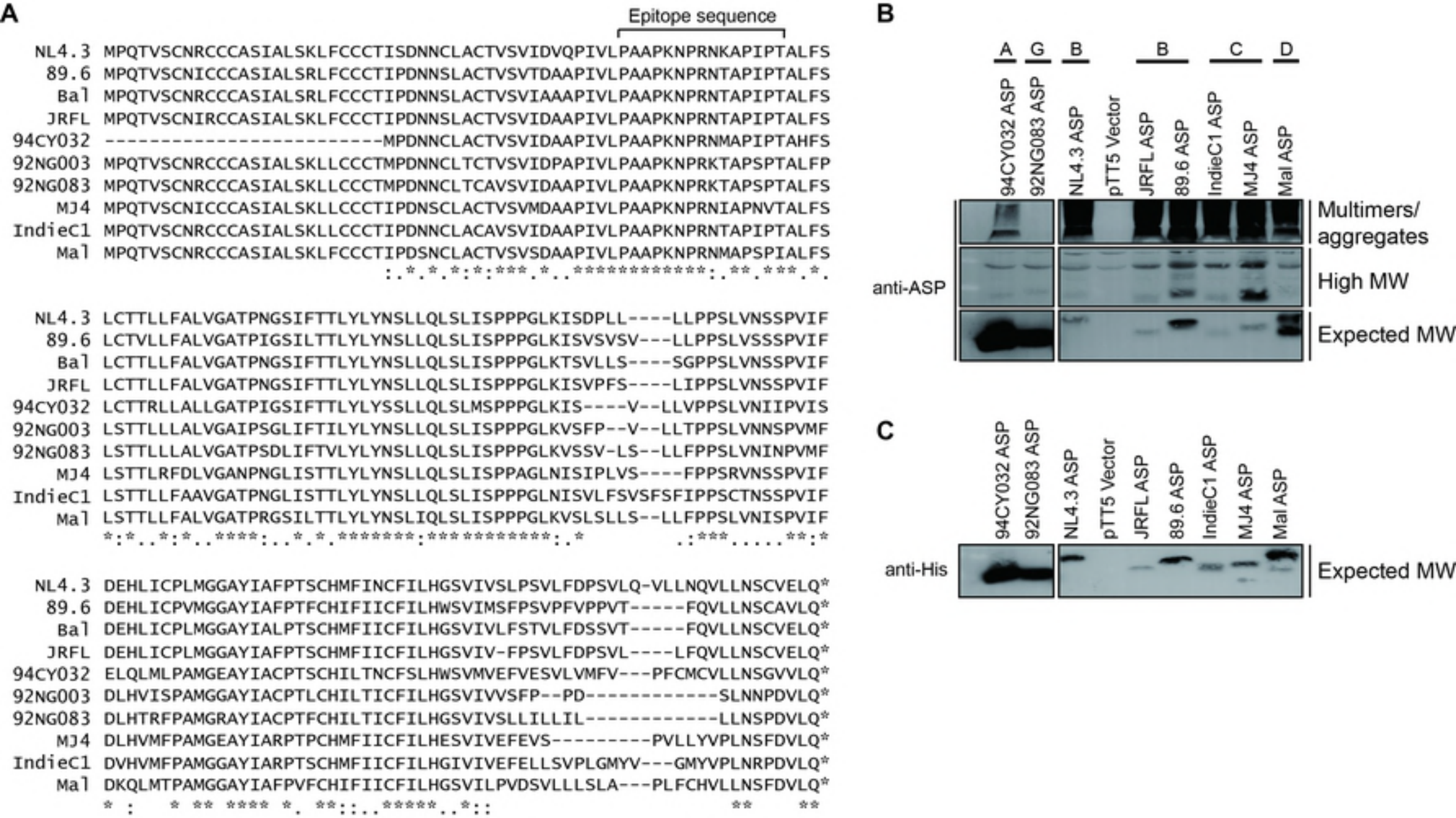
A
Epitope sequence
NL4.3 MPQTVSCNRCCCASIALSKLFCCCTISDNNCLACTVSVIDVQPIVLPAAPKNPRNKAPIPTALFS
89.6 MPQTVSCNICCCASIALSRLFCCCTIPDNNSLACTVSVTDAAPIVLPAAPKNPRNTAPIPTALFS
Bal MPQTVSCNRCCCASIALSRLFCCCTIPDNNSLACTVSVIAAAPIVLPAAPKNPRNTAPIPTALFS
JRFL MPQTVSCNIRCCASIALSKLFCCCTIPDNNSLACTVSVIDAAPIVLPAAPKNPRNTAPIPTALFS
94CY032 ----------MPDNNCLACTVSVIDAAPIVLPAAPKNPRNMAPIPTAHFS
92NG003 MPQTVSCNRCCCASIALSKLLCCCTMPDNNCLTCTVSVIDPAPIVLPAAPKNPRKTAPSPTALFP
92NG083 MPQTVSCNRCCCASIALSKLLCCCTMPDNNCLTCAVSVIDAAPIVLPAAPKNPRKTAPSPTALFS
MJ4 MPQTVSCNICCCASIALSKLLCCCTIPDNSCLACTVSVMDAAPIVLPAAPKNPRNIAPNVTALFS
IndieC1 MPQTVSCNRCCCASIALSKLLCCCTIPDNNCLACAVSVIDAAPIVLPAAPKNPRNTAPIPTALFS
Mal MPQTVSCNRCCCASIALSKLFCCCTIPDSNCLACTVSVSDAAPIVLPAAPKNPRNMAPSPIALFS
NL4.3 LCTTLLFALVGATPNGSIFTTLYLYNSLLQLSLISPPPGLKISDPLL----LLPPSLVNSSPVIF
89.6 LCTVLLFALVGATPIGSILTTLYLYNSLLQLSLISPPPGLKISVSVSV---LLPPSLVSSSPVIF
Bal LCTTLLFALVGATPNGSIFTTLYLYNSLLQLSLISPPPGLKTSVLLS----SGPPSLVNSSPVIF
JRFL LCTTLLFALVGATPNGSIFTTLYLYNSLLQLSLISPPPGLKISVPFS----LIPPSLVNSSPVIF
94CY032 LCTTRLLALLGATPIGSIFTTLYLYSSLLQLSLMSPPPGLKIS----V--LLVPPSLVNIIPVIS
92NG003 LSTTLLLALVGAIPSGLIFTILYLYNSLLQLSLISPPPGLKVSFP--V--LLTPPSLVNNSPVMF
92NG083 LSTTLLLALVGATPSDLIFTVLYLYNSLLQLSLISPPPGLKVSSV-LS--LLFPPSLVNINPVMF
MJ4 LSTTLRFDLVGANPNGLISTTLYLYNSLLQLSLISPPAGLNISIPLVS----FPPSRVNSSPVIF
IndieC1 LSTTLLFAAVGATPNGLISTTLYLYNSLLQLSLISPPPGLNISVLFSVSFSFIPPSCTNSSPVIF
Mal LSTTLLFALVGATPRGSILTTLYLYNSLIQLSLISPPPGLKVSLSLLS--LLFPPSLVNISPVIF
NL4.3 DEHLICPLMGGAYIAFPTSCHMFINCFILHGSVIVSLPSVLFDPSVLQ-VLLNQVLLNSCVELQ*
89.6 DEHLICPVMGGAYIAFPTFCHIFIICFILHWSVIMSFPSVPFVPPVT-----FQVLLNSCAVLQ*
Bal DEHLICPLMGGAYIALPTSCHMFIICFILHGSVIVLFSTVLFDSSVT-----FQVLLNSCVELQ*
JRFL DEHLICPLMGGAYIAFPTSCHMFIICFILHGSVIV-FPSVLFDPSVL----LFQVLLNSCVELQ*
94CY032 ELQLMLPAMGEAYIACPTSCHILTNCFSLHWSVMVEFVESVLVMFV---PFCMCVLLNSGVVLQ*
92NG003 DLHVISPAMGGAYIACPTLCHILTICFILHGSVIVVSFP--PD----------SLNNPDVLQ*
92NG083 DLHTRFPAMGRAYIACPTFCHILTICFILHGSVIVSLLILLIL----------LLNSPDVLQ*
MJ4 DLHVMFPAMGEAYIARPTPCHMFIICFILHESVIVEFEVS---------PVLLYVPLNSFDVLQ*
IndieC1 DVHVMFPAMGGAYIARPTSCHMFIICFILHGIVIVEFELLSVPLGMYV---GMYVPLNRPDVLQ*
Mal DKQLMTPAMGGAYIAFPVFCHIFIICFILHGSVILPVDSVLLLSLA---PLFCHVLLNSFDVLQ*
B
A
G
B
B
C
D
94CY032 ASP
92NG083 ASP
NL4.3 ASP
pTT5 Vector
JRFL ASP
89.6 ASP
IndieC1 ASP
MJ4 ASP
Mal ASP
anti-ASP
Multimers/ aggregates
High MW
Expected MW
C
94CY032 ASP
92NG083 ASP
NL4.3 ASP
pTT5 Vector
JRFL ASP
89.6 ASP
IndieC1 ASP
MJ4 ASP
Mal ASP
anti-His
Expected MW

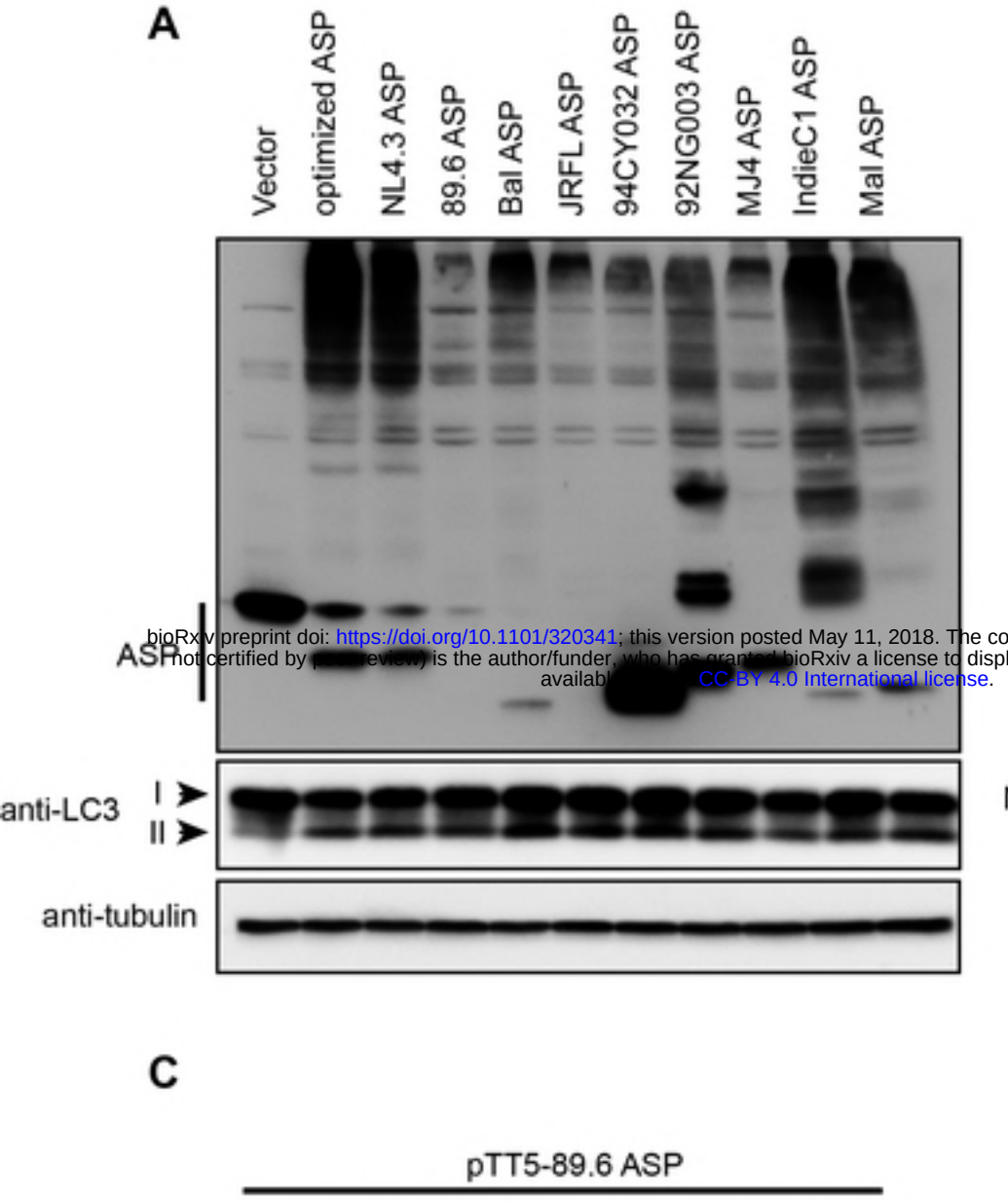

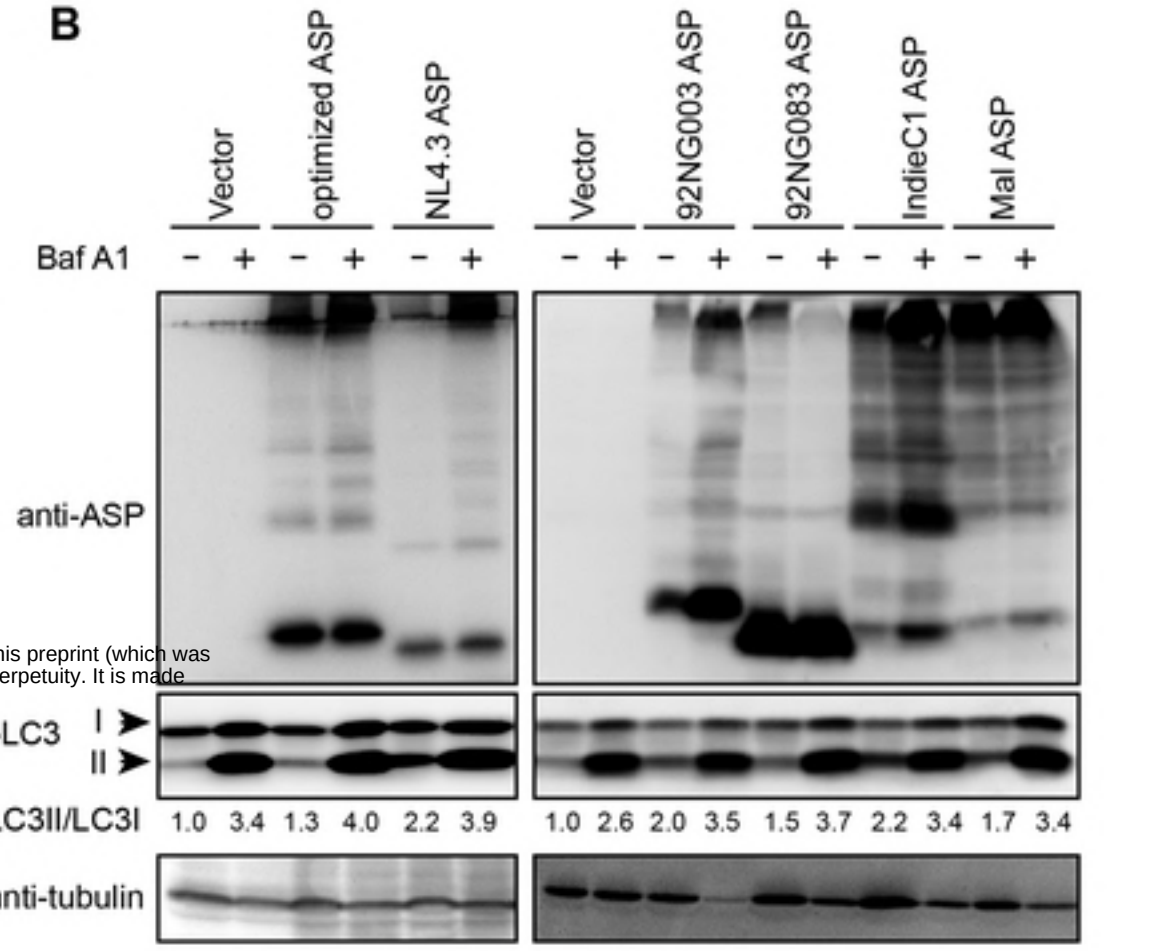

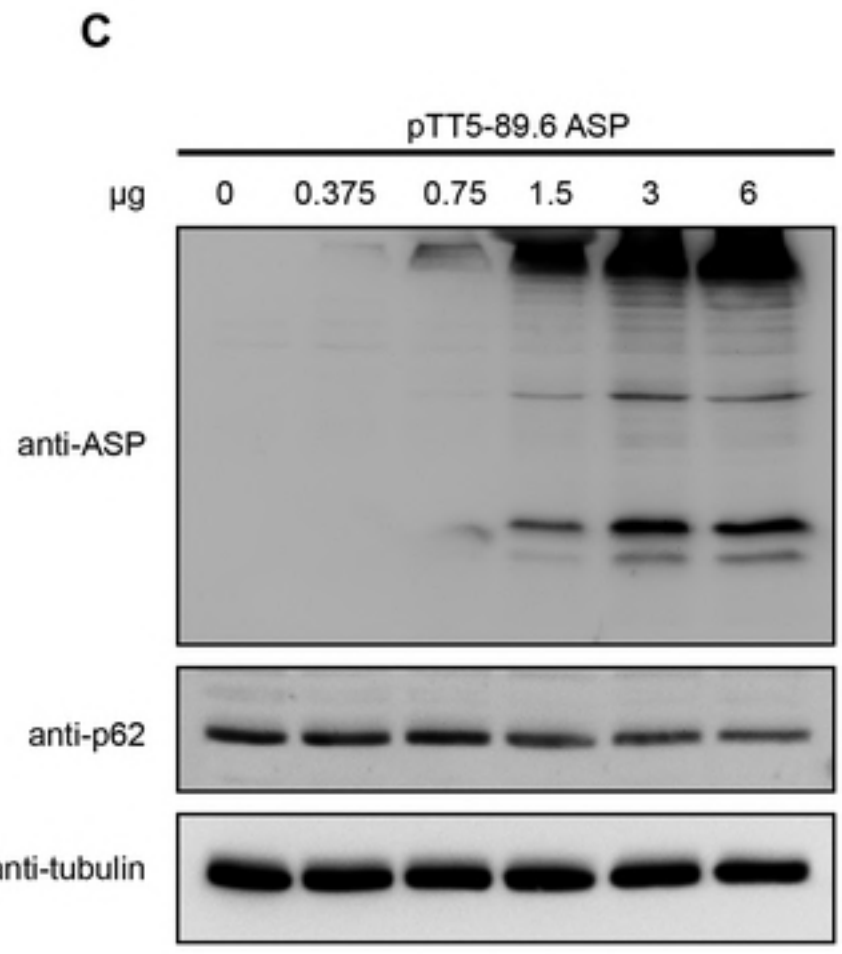

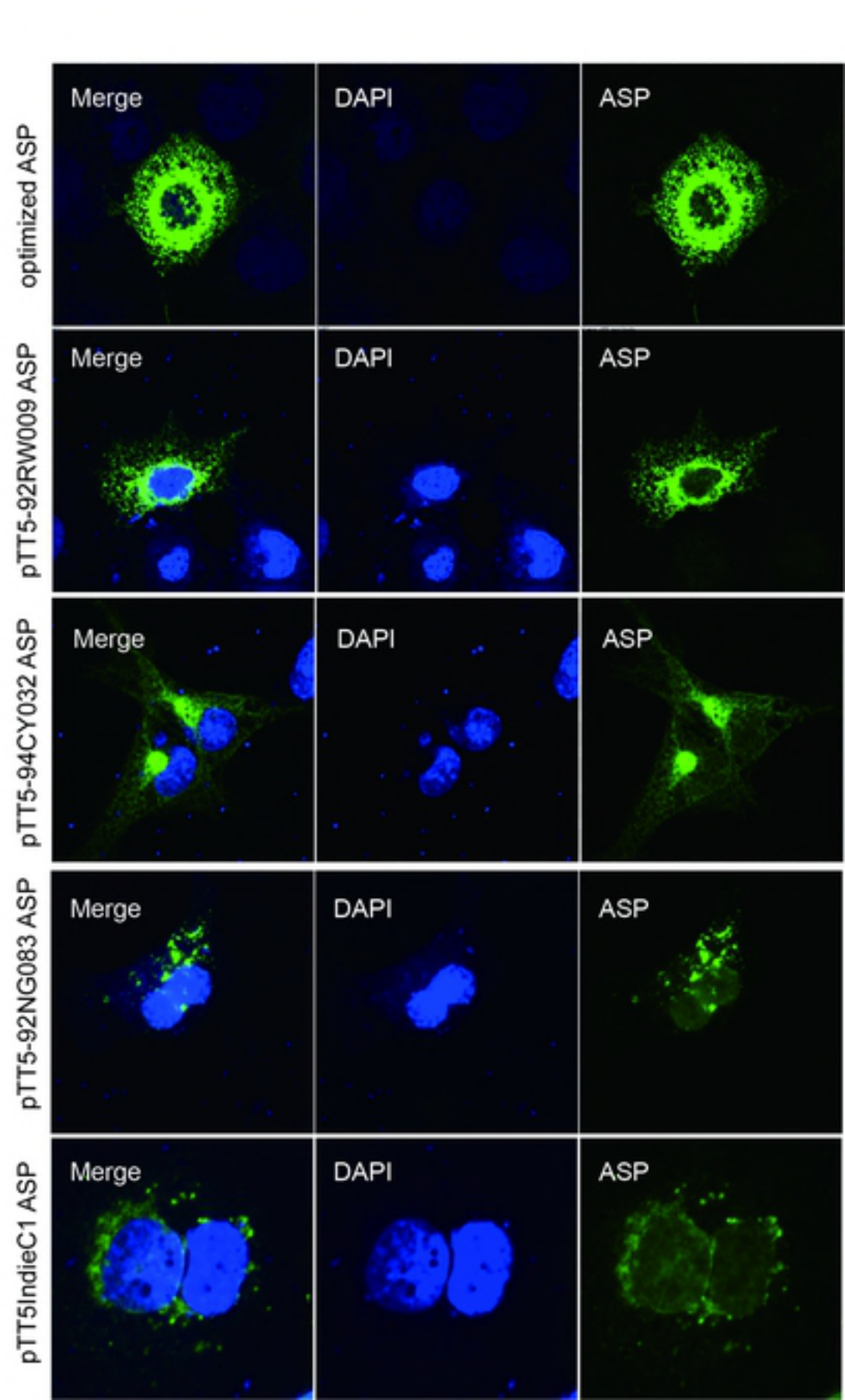

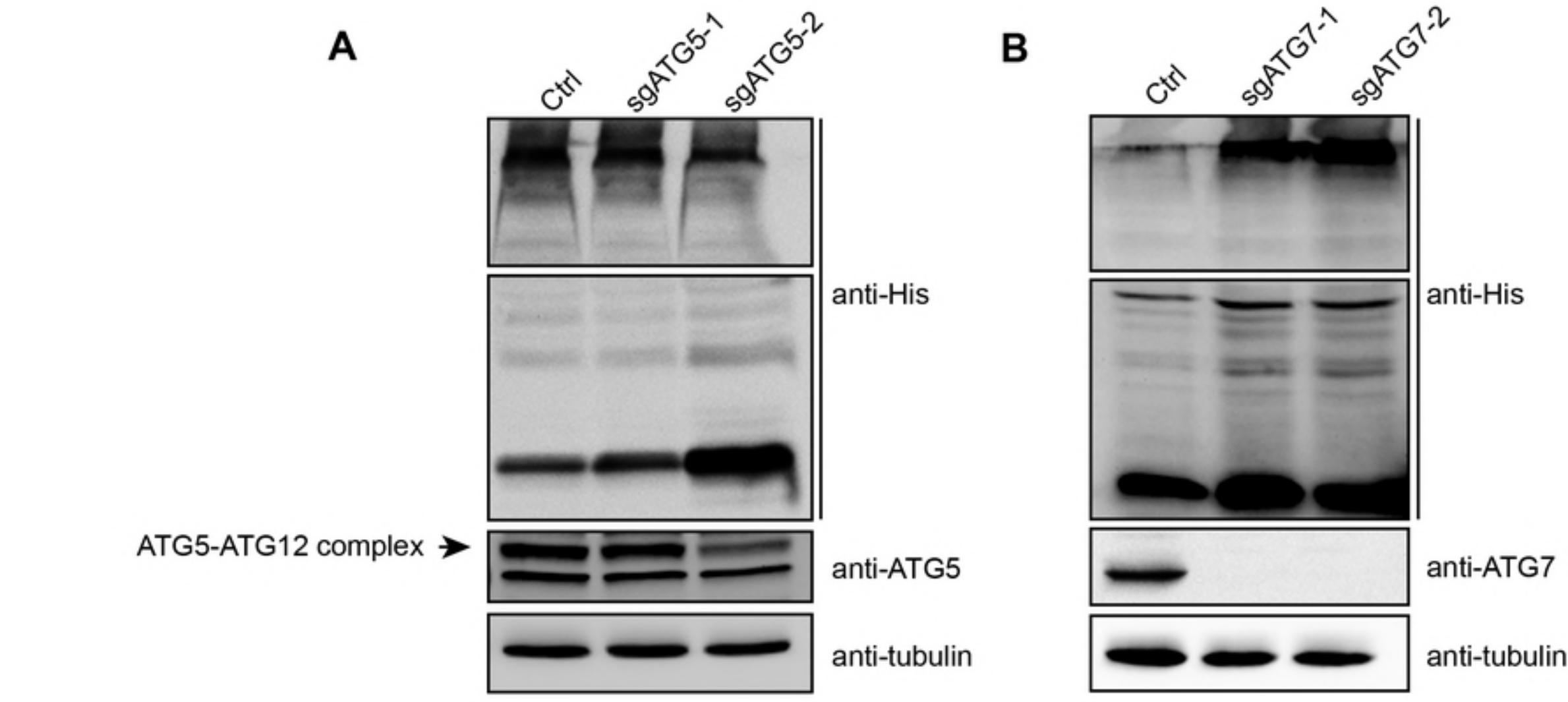
A
Ctrl
sgATG5-1
sgATG5-2
anti-His
ATG5-ATG12 complex
anti-ATG5
anti-tubulin
B
Ctrl
sgATG7-1
sgATG7-2
anti-His
anti-ATG7
anti-tubulin

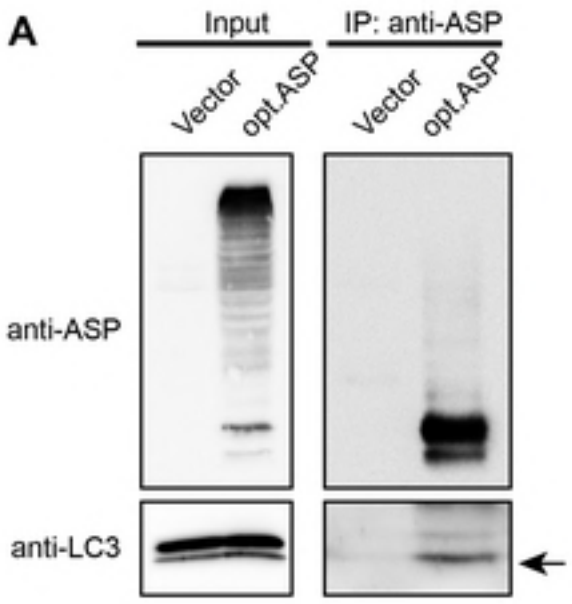

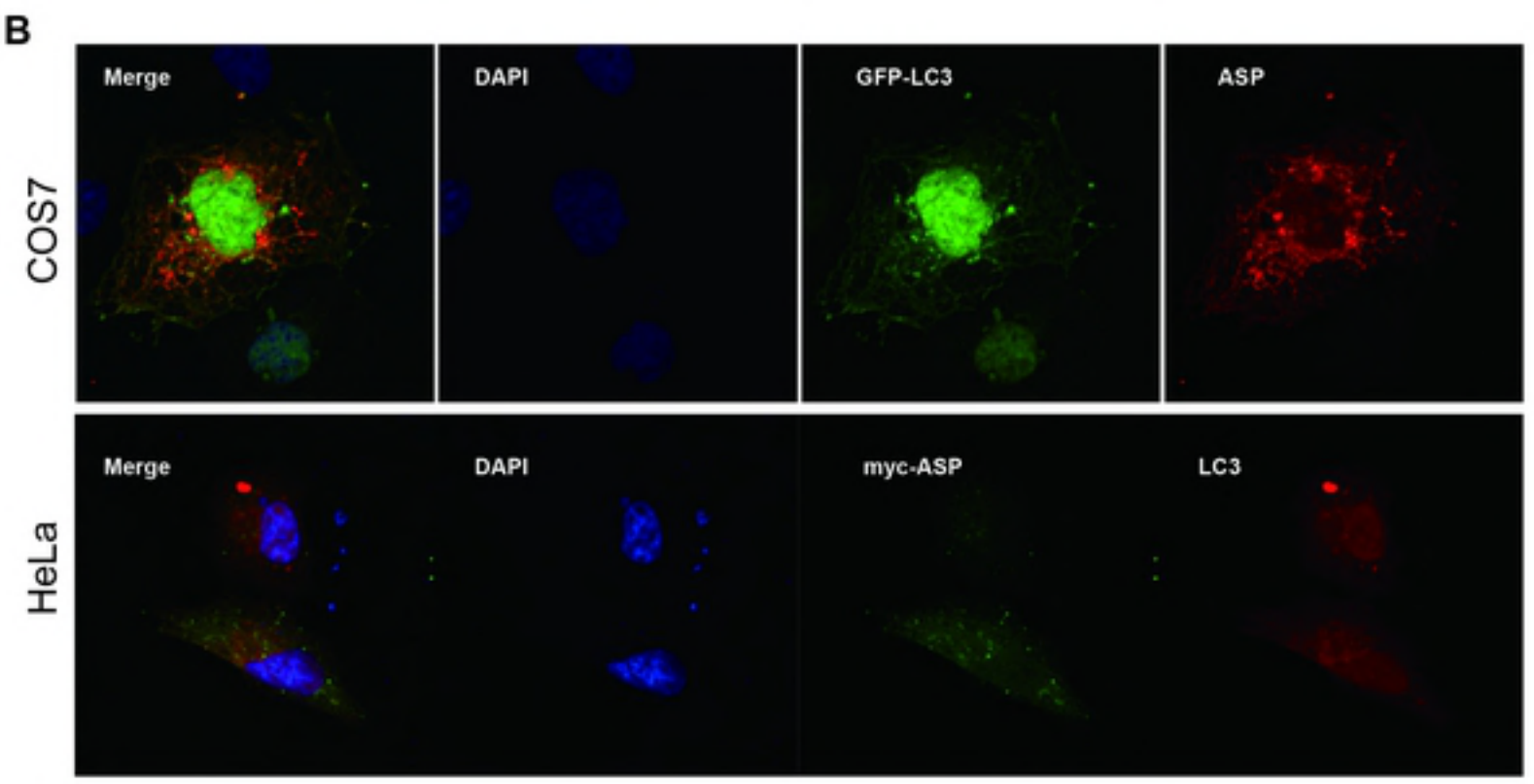

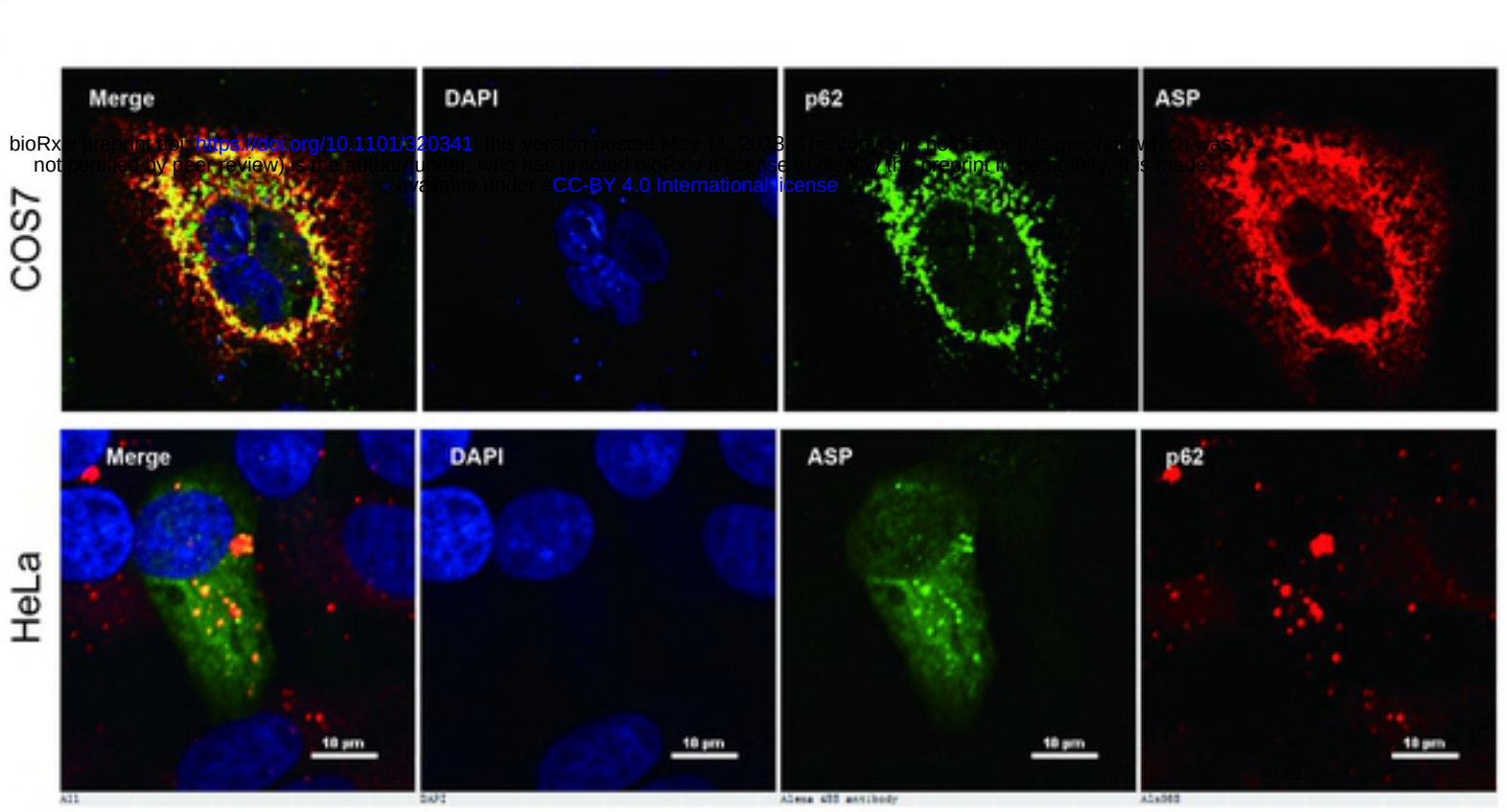

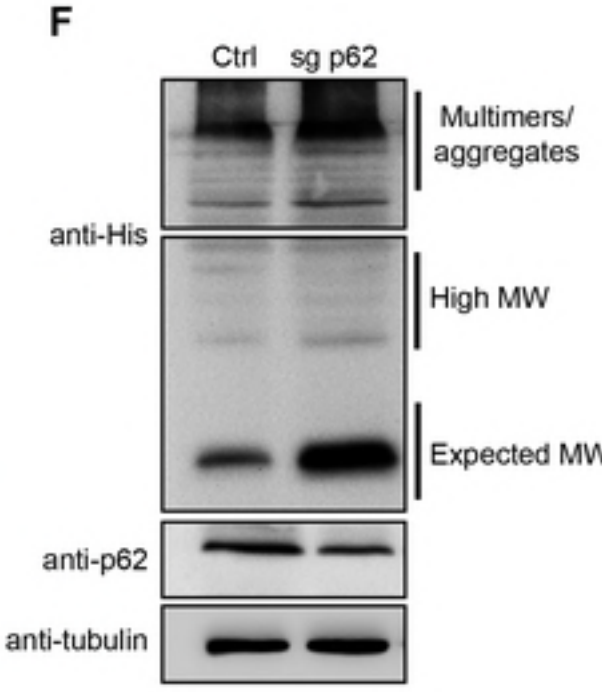

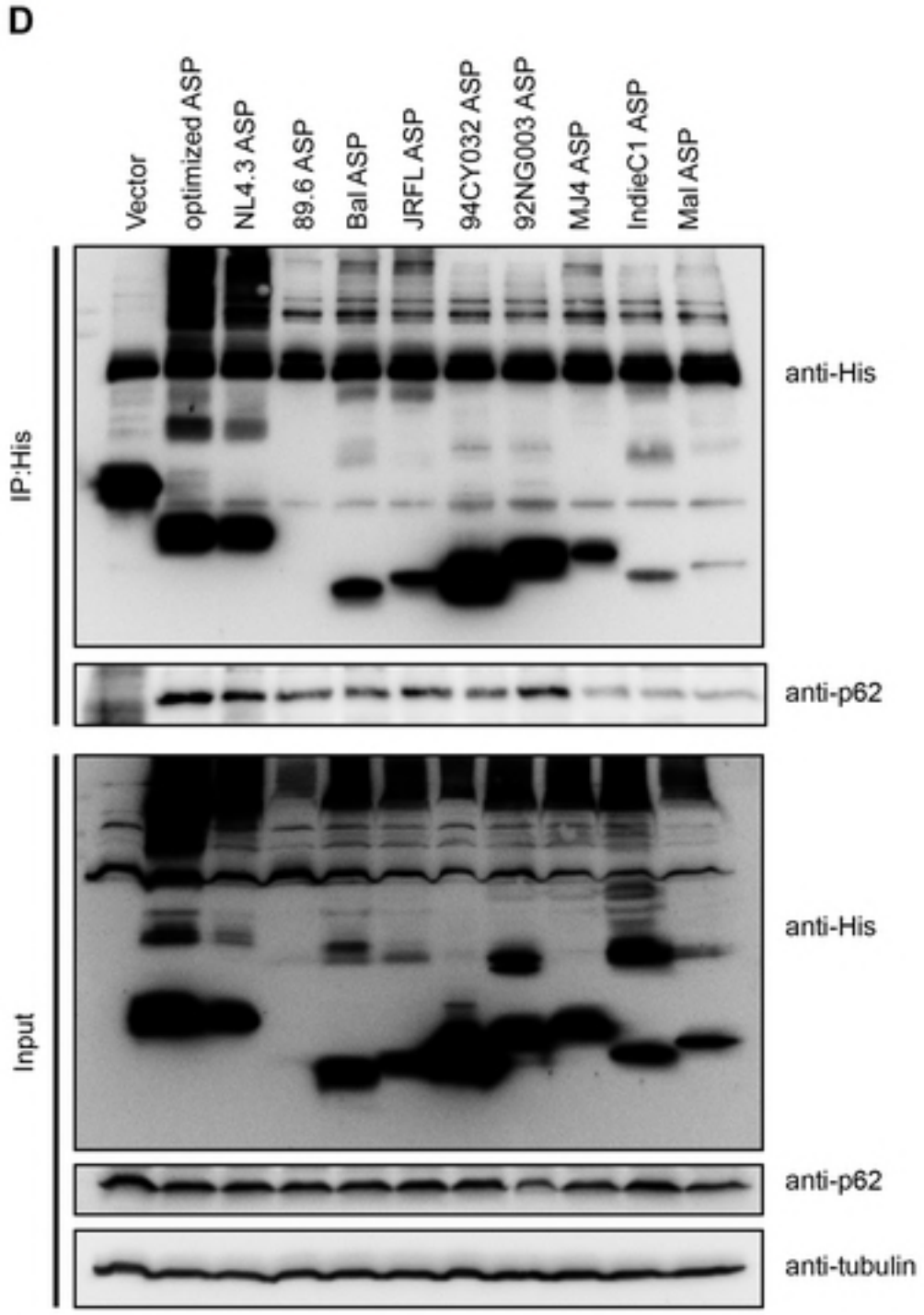

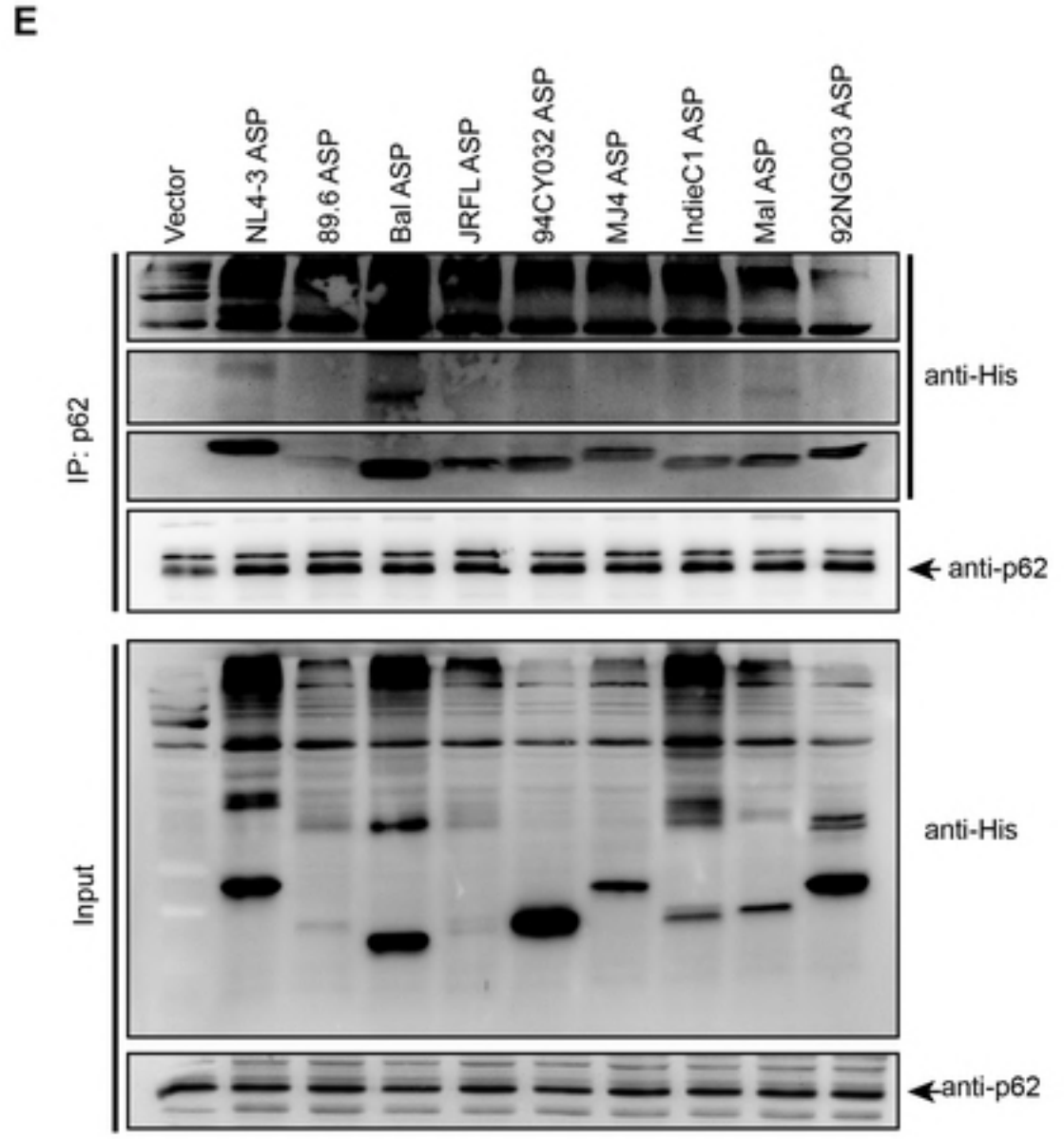

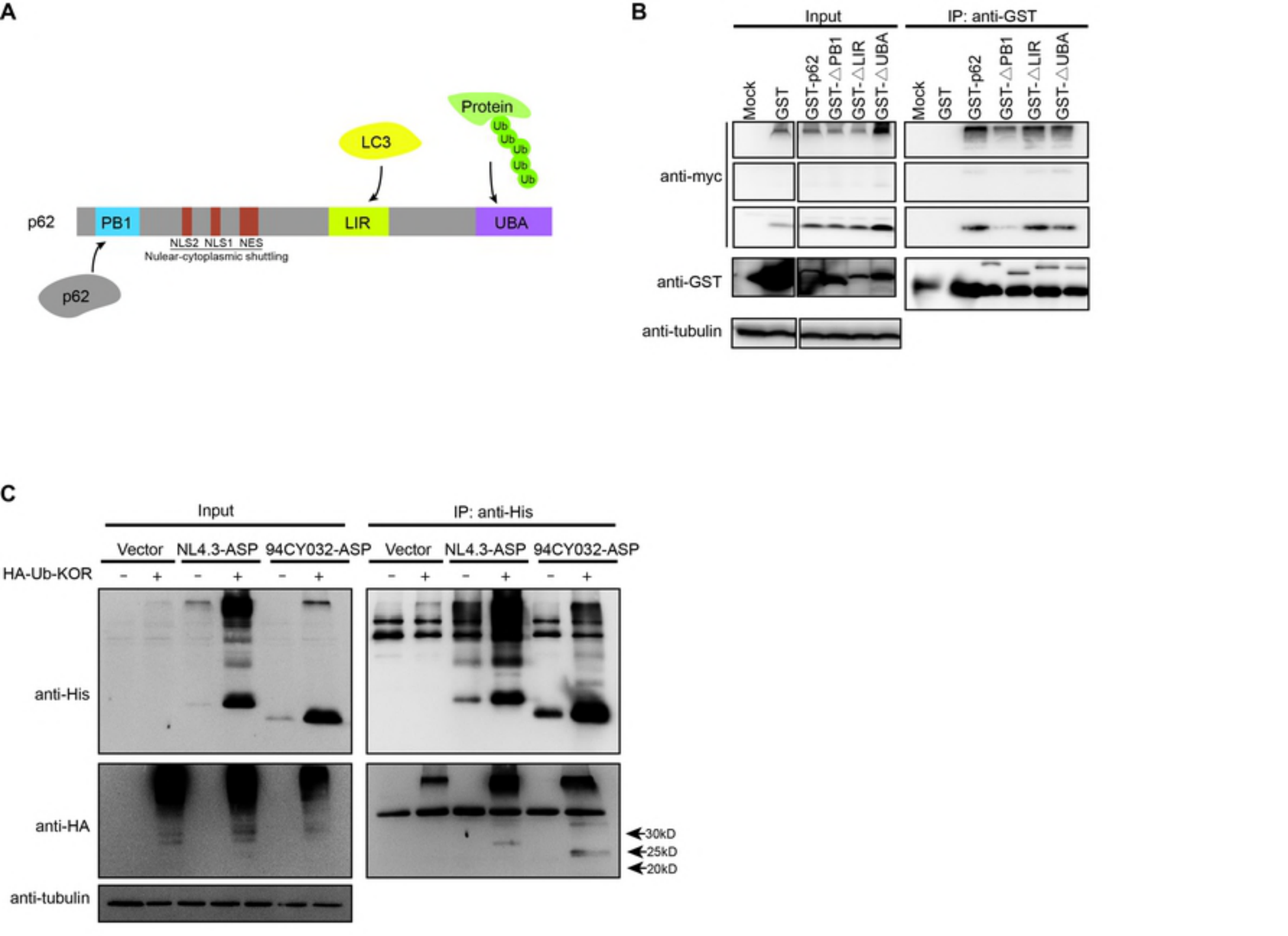
A
Protein
Ub
Ub
Ub
Ub
Ub
LC3
p62
PB1
LIR
UBA
NLS2 NLS1 NES
Nulear-cytoplasmic shuttling
p62
B
Input
IP: anti-GST
Mock
GST
GST-p62
GST-△PB1
GST-△LIR
GST-△UBA
Mock
GST
GST-p62
GST-△PB1
GST-△LIR
GST-△UBA
anti-myc
anti-GST
anti-tubulin
C
Input
IP: anti-His
Vector
NL4.3-ASP
94CY032-ASP
Vector
NL4.3-ASP
94CY032-ASP
HA-Ub-KOR
- + - + - + - + - + - +
anti-His
anti-HA
anti-tubulin
30kD
25kD
20kD